

# Dynamic targeting enables domain-general inhibitory control over action and thought by the prefrontal cortex

Dace Apšvalka<sup>1\*</sup>, Catarina S. Ferreira<sup>2\*</sup>, Taylor W. Schmitz<sup>3</sup>, James B. Rowe<sup>1,4</sup>, Michael C. Anderson<sup>1,5</sup>

<sup>1</sup> MRC Cognition and Brain Sciences Unit, University of Cambridge, Cambridge, UK

<sup>2</sup> School of Psychology, University of Birmingham, Birmingham, UK

<sup>3</sup> Brain and Mind Institute, Western University, London, Ontario, Canada

<sup>4</sup> University of Cambridge, Department of Clinical Neurosciences, Cambridge, UK

<sup>5</sup> University of Cambridge, Behavioural and Clinical Neuroscience Institute, Cambridge, UK

October 23, 2020. Preprint v1.1

Successful self-control requires the ability to stop unwanted actions or thoughts. Stopping is regarded as a central function of inhibitory control, a mechanism enabling the suppression of diverse mental content, and strongly associated with the prefrontal cortex. A domain-general inhibitory control capacity, however, would require the region or regions implementing it to dynamically shift top-down inhibitory connectivity to diverse target regions in the brain. Here we show that stopping unwanted thoughts and stopping unwanted actions engage common regions in the right anterior dorsolateral and right ventrolateral prefrontal cortex, and that both areas exhibit this dynamic targeting capacity. Within each region, pattern classifiers trained to distinguish stopping actions from making actions also could identify when people were suppressing their thoughts (and vice versa) and could predict which people successfully forgot thoughts after inhibition. Effective connectivity analysis revealed that both regions contributed to action and thought stopping, by dynamically shifting inhibitory connectivity to motor area M1 or to the hippocampus, depending on the goal, suppressing task-specific activity in those regions. These findings support the existence of a domain-general inhibitory control mechanism that contributes to self-control and establish dynamic inhibitory targeting as a key mechanism enabling these abilities.

## Introduction

Well-being during difficult times requires the ability to stop unwelcome thoughts. This vital ability may be grounded in inhibitory control mechanisms that also stop physical actions (Anderson & Hanslmayr, 2014; Anderson et al., 2004; Castiglione et al., 2019; Depue et al., 2016; Depue et al., 2007). According to this hypothesis, the right lateral prefrontal cortex (rLPFC) supports self-control, allowing people to regulate their thoughts and behaviours when

fears, ruminations, or impulsive actions might otherwise hold sway (Anderson & Hulbert, 2021; Benoit et al., 2016; Schmitz et al., 2017). This proposal rests on the concept of inhibitory control, a putative domain-general control mechanism that has attracted much interest in psychology and neuroscience over the last two decades (Anderson et al., 2016; Aron et al., 2004, 2014; Banich & Depue, 2015; Bari & Robbins, 2013; Boucher et al., 2007; Diamond, 2013; Ersche et al., 2012; Eysenck et al., 2007; Joormann & Tanovic, 2015; Lipszyc & Schachar, 2010). Despite widespread and enduring interest, central evidence for the neural basis of domain-general inhibitory control is missing: no study has shown a control region that dynamically shifts its connectivity to suppress local processing in diverse cortical areas depending on the stopping goal – a fundamental capability of this putative mechanism. Inhibiting actions and memories, for example, requires that an inhibitory control region target disparate specialised brain areas to suppress motoric or mnemonic processing, respectively. We term this predicted capability dynamic targeting. Here, we tested the existence of dynamic targeting by asking participants to stop unwanted actions or thoughts. Using functional magnetic resonance imaging (fMRI) and pattern classification, we identified prefrontal regions that contribute to successful stopping in both domains. Critically, we then tested whether people's intentions to stop actions or thoughts were reflected in altered effective connectivity between the domain-general inhibition regions in prefrontal cortex with memory or motor-cortical areas. By tracking the dynamic targeting of inhibitory control in the brain, we provide a window into humans' capacity for self-control over their thoughts and behaviours (Nigg, 2017).

Our analysis builds on evidence that two regions of the rLPFC may contribute to stopping both actions and thoughts: the right ventrolateral prefrontal cortex (rVLPFC) and the right dorsolateral prefrontal cortex (rDLPFC). For example, stopping motor actions activates

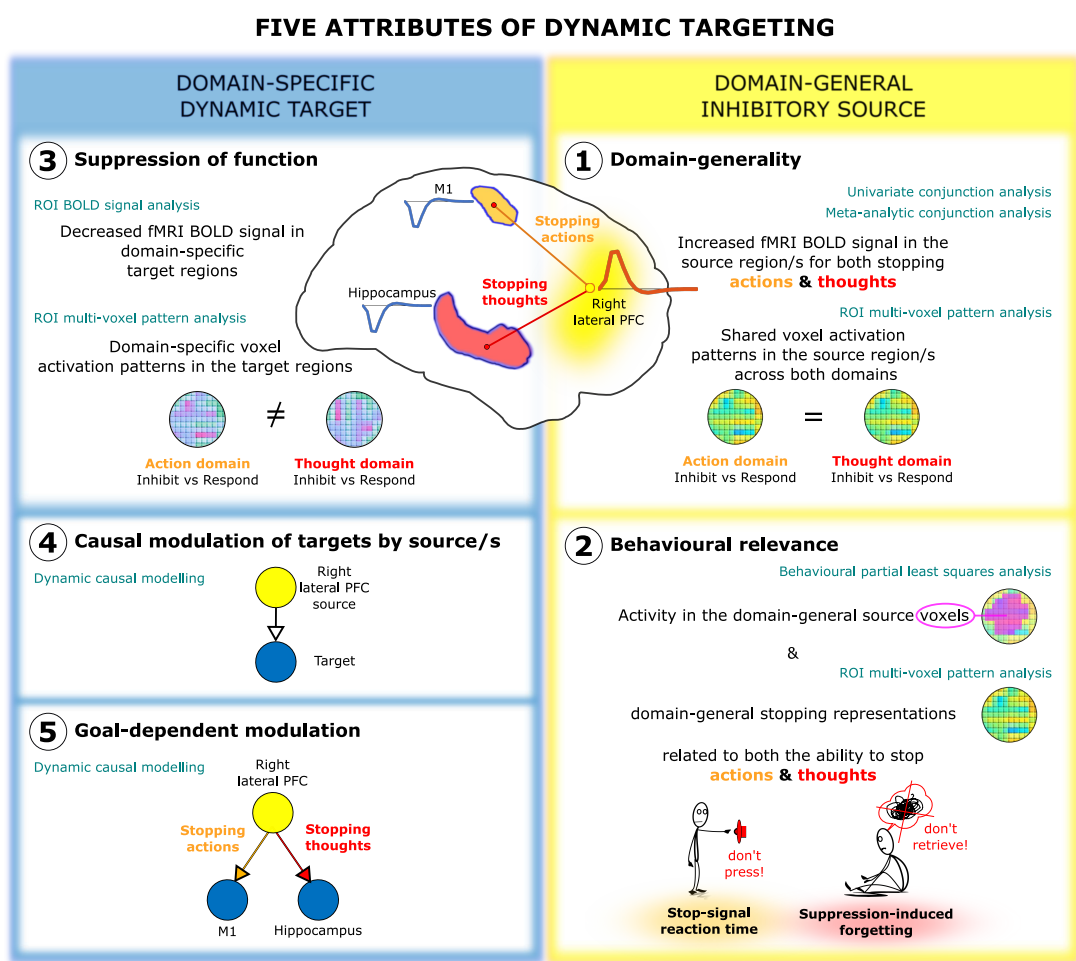


**Figure 1. Five attributes of dynamic targeting.** Schematic of the five attributes of domain-general inhibitory control by dynamic targeting and methods employed (teal colour) to test the attributes. Attributes 1-2 relate to the existence of domain-general inhibitory sources. The predicted location of such sources was in the right lateral PFC. We present the two attributes on the right side to match the visualised location of the expected sources. To test the domain-generality of inhibitory sources (attribute 1), we performed univariate and meta-analytic conjunction analysis of the No-Think > Think and Stop > Go contrasts, and cross-task multi-voxel pattern analysis (MVPA). To test the behavioural relevance (attribute 2), we related inhibitory activations within the identified domain-general regions to individual variation in inhibition ability (stop-signal reaction time and suppression-induced forgetting) using behavioural partial-least squares and MVPA. Attributes 3-5 relate to the existence of domain-specific target sites that are dynamically modulated by the domain-general sources. Our a priori assumption was that suppressing actions and thoughts would target M1 and hippocampus, respectively. To test the suppression of function within the target sites (attribute 3) we performed a region of interest (ROI) analysis expecting down-regulation within the target sites, and cross-task MPVA expecting distinct activity patterns across the two task domains. To test whether the prefrontal domain-general sources exert top-down modulation of the target sites (attribute 4) dynamically targeting M1 or the hippocampus depending on the process being stopped (attribute 5), we performed dynamic causal modelling.

1 rVLPFC (especially in BA44/45, pars opercularis), rDLPFC, 16  
 2 and anterior insula (Aron et al., 2004; Guo et al., 2018; 17  
 3 Jahanshahi et al., 2015; Levy & Wagner, 2011; Rae et al., 18  
 4 2014; Zhang et al., 2017). Disrupting rVLPFC impairs 19  
 5 motor inhibition, whether via lesions (Aron et al., 2003), 20  
 6 transcranial magnetic stimulation (Chambers et al., 2006), 21  
 7 intracranial stimulation in humans (Wessel et al., 2013) or 22  
 8 monkeys (Sasaki et al., 1989). rVLPFC thus could promote 23  
 9 top-down inhibitory control over actions, and possibly in- 24  
 10 hibitory control more broadly (Aron, 2007; Aron et al., 25  
 11 2004; Castiglione et al., 2019). Within-subjects compar- 26  
 12 isions have identified shared activations in rDLPFC (BA 27  
 13 9/46) that could support a domain-general mechanism 28  
 14 that stops both actions and thoughts (Depue et al., 2016). 29  
 15 If these rLPFC regions support domain-general in-

hibitory control, the question arises as to how inhibition is directed at actions or thoughts. To address this issue, we tested whether any regions within the rLPFC had the dynamic targeting capacity needed to support domain-general inhibitory control. Dynamic targeting requires that a candidate inhibitory control system exhibit five core attributes (see Figure 1). First, stopping in diverse domains should engage the proposed source of control, with activation patterns within this region transcending the specific demands of each stopping type. As a consequence, activation patterns during any one form of stopping should contain information shared with inhibition in other domains. Second, the engagement of the proposed prefrontal source should track indices of inhibitory control in diverse domains, demonstrating its behavioural relevance. Third,

1 stopping-related activity in the prefrontal sources should 59  
2 co-occur with interrupted functioning in domain-specific 60  
3 target sites representing thoughts or actions. Fourth, the 61  
4 prefrontal source should exert top-down inhibitory cou- 62  
5 pling with these target sites, providing the causal basis of 63  
6 their targeted suppression. Finally, dynamic targeting re- 64  
7 quires that inhibitory coupling between prefrontal source 65  
8 and domain-specific target regions be selective to current 66  
9 goals. 67

10 These attributes of dynamic targeting remain unproven, 68  
11 despite the fundamental importance of inhibitory control. 69  
12 Research on response inhibition and thought suppression 70  
13 instead has focused on how the prefrontal cortex con- 71  
14 tributes to stopping within each domain (Anderson et al., 72  
15 2016; Jana et al., 2020; Schall et al., 2017; Wiecki & 73  
16 Frank, 2013). For example, research on thought suppres- 74  
17 sion has revealed top-down inhibitory coupling from the 75  
18 rDLPFC to the hippocampus, and to several cortical regions 76  
19 representing specific mnemonic content (Benoit & Ander- 77  
20 son, 2012; Benoit et al., 2015; Gagnepain et al., 2014; 78  
21 Gagnepain et al., 2017; Mary et al., 2020; Schmitz et al., 79  
22 2017). Moreover, suppressing thoughts down-regulates 80  
23 hippocampal activity, with the down-regulation linked 81  
24 to hippocampal GABA and forgetting of the suppressed 82  
25 content (Schmitz et al., 2017). Top-down modulation of 83  
26 actions by rVLPFC suggests that premotor and primary mo- 84  
27 tor cortex are target sites (Aron & Poldrack, 2006; Rae et 85  
28 al., 2015; Zandbelt et al., 2013). Action stopping engages 86  
29 local intracortical inhibition within M1 to achieve stop- 87  
30 ping (Coxon et al., 2006; Sohn et al., 2002; Stinear et al., 88  
31 2009; van den Wildenberg et al., 2010), with a person's 89  
32 stopping efficacy related to local GABAergic inhibition (He 90  
33 et al., 2019). However, studies of thought suppression and 91  
34 action stopping posit that control originates from different 92  
35 prefrontal regions (rDLPFC vs rVLPFC), possibly reflecting 93  
36 domain-specific inhibitory control mechanisms. A can- 94  
37 didate source of domain-general inhibitory control must 95  
38 stop both actions and thoughts and exhibit the attributes 96  
39 of dynamic targeting. 97

40 Although dynamic inhibitory targeting has not been 98  
41 tested, some large-scale networks flexibly shift their cou- 99  
42 pling with diverse brain regions that support task per- 100  
43 formance. Diverse tasks engage a fronto-parietal net- 101  
44 work (Cole et al., 2013; Cole & Schneider, 2007; Duncan, 102  
45 2010; Fox et al., 2005), which exhibits greater cross-task 103  
46 variability in coupling with other regions than other net- 104  
47 works (Cocuzza et al., 2020; Cole et al., 2013). Variable 105  
48 connectivity may index this network's ability to recon- 106  
49 figure flexibly and coordinate multiple task elements in 107  
50 the interests of cognitive control (Cole et al., 2013). A 108  
51 cingulo-opercular network, including aspects of rDLPFC 109  
52 and rVLPFC, also is tied to cognitive control, including 110  
53 conflict and attentional processing (Botvinick, 2007; Cole 111  
54 et al., 2009; Crittenden et al., 2016; Dosenbach et al., 112  
55 2006; Petersen & Posner, 2012; Seeley et al., 2007; Yeo et 113  
56 al., 2015), with the prefrontal components exhibiting high 114  
57 connectivity variability over differing tasks (Cocuzza et al., 115  
58 2020). However, previous analyses of these networks do 116

not address dynamic inhibitory targeting: Dynamic targeting requires not merely that the prefrontal cortex exhibits connectivity to multiple regions, but that the connectivity includes a top-down component that suppresses target regions.

We sought to test the presence of dynamic targeting through the properties of prefrontal, motor and hippocampal networks (see Figure 1 for an overview of our approach). We combined, within one fMRI session, a cognitive manipulation to suppress unwanted thoughts, the Think/No-Think paradigm (Anderson & Green, 2001; Anderson & Hulbert, 2021), with motor action stopping in a stop-signal task (Logan & Cowan, 1984; Verbruggen et al., 2019). This design provided the opportunity to identify co-localized activations of domain-general inhibitory control in prefrontal sources and observe their changes in effective connectivity with motor cortical and hippocampal targets. For the thought suppression task, prior to scanning, participants learned word pairs, each composed of a reminder and a paired thought (Figure 2). During thought stopping scanning blocks, on each trial, participants viewed one of these reminders. For each reminder, we cued participants either to retrieve its associated thought (Think trials) or instead to suppress its retrieval, stopping the thought from coming to mind (No-Think trials). For the action stopping task, prior to scanning, participants were trained to press one of two buttons in response to differently coloured circles (Schmitz et al., 2017). During the action stopping scanning blocks, participants engaged in a speeded motor response task that, on a minority of trials, required them to stop their key-press following an auditory stop signal. Action and thought stopping blocks alternated, to enable quantification of domain-general and domain-specific activity and connectivity.

The dynamic targeting hypothesis predicts that stopping actions and thoughts call upon a common inhibition mechanism. For thought suppression, we predicted that the reminder would activate the associated thought, triggering inhibitory control to suppress hippocampal retrieval (Anderson et al., 2004; Levy & Anderson, 2012). We predicted that this disruption would hinder later retrieval of the thought, causing suppression-induced forgetting. To verify this, we tested all pairs (both Think and No-Think pairs) after scanning, including a group of pairs that had been learned, but that were omitted during the Think/No-Think task, to estimate baseline memory performance (Baseline pairs). Suppression-induced forgetting occurs when final recall of No-Think items is lower than Baseline items (Anderson & Green, 2001). For action stopping, we proposed that the Go stimulus would rapidly initiate action preparation, with the presentation of the stop signal triggering inhibitory control to suppress motor processes in M1 (Logan & Cowan, 1984; Verbruggen et al., 2019). If the capacities to stop actions and thoughts are related, more efficient action stopping, as measured by stop-signal reaction time, should correlate with greater suppression-induced forgetting.

Our primary goal was to determine whether any pre-

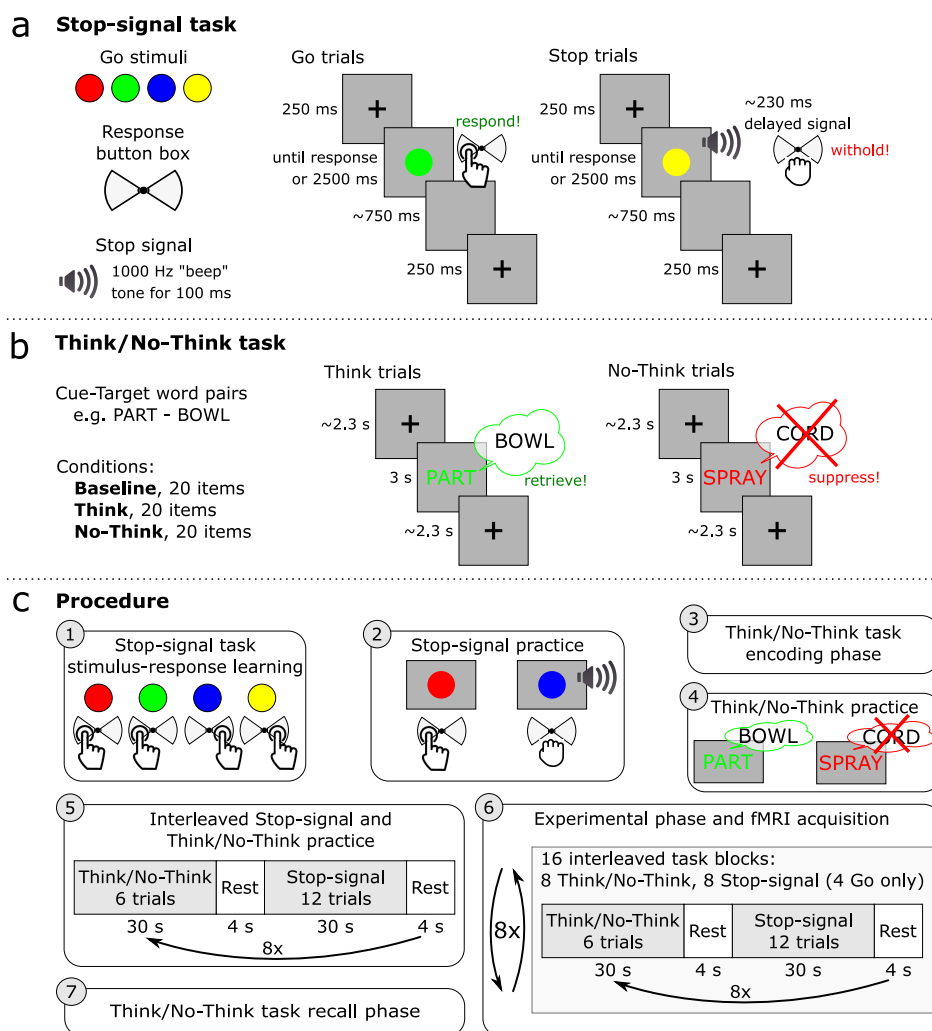


**Figure 2. Schematic of the experimental paradigm and procedure.** (a) In the Stop-signal task, the Go stimuli were red, green, blue, and yellow coloured circles. On Go trials, participants responded by pressing one of the two buttons on a button box according to learned stimulus-response associations. On Stop trials, shortly after the Go stimulus, an auditory "beep" tone would signal participants to withhold the button press. The stop-signal delay varied dynamically in 50 ms steps to achieve approximately a 50% success-to-stop rate for each participant. (b) In the Think/No-Think task, participants learned 78 cue-target word pair associations. Sixty of the word pairs were then divided into three lists composed of 20 items each and allocated to the three experimental conditions: Think, No-Think, and Baseline. During Think trials, a cue word appeared in green, and participants had 3 s to retrieve and think of the associated target word. On No-Think trials, a cue word appeared in red and participants were asked to suppress the retrieval of the associated target word and push it out of awareness if it popped into their mind. (c) The procedure consisted of 7 steps: 1) stimulus-response learning for the Stop-signal task; 2) Stop-signal task practice; 3) encoding phase of the Think/No-Think task; 4) Think/No-Think practice; 5) practice of interleaved Stop-signal and Think/No-Think tasks; 6) the main experimental phase during fMRI acquisition where participants performed interleaved 30 s blocks of Stop-signal and Think/No-Think tasks; 7) recall phase of the Think/No-Think task.

frontal source region meets the five core attributes for dynamic targeting of inhibitory control. To test this, we first identified candidate regions that could serve as sources of control. We isolated prefrontal regions that were more active during action and thought stopping, compared to their respective control conditions (e.g. "Go" trials, wherein participants made the cued action; or Think trials, wherein they retrieved the cued thought) and then performed a within-subjects conjunction analysis on these activations. We performed a parallel conjunction analysis on independent data from two quantitative meta-analyses of fMRI studies that used the Stop-signal or the Think/No-Think tasks, to confirm the generality of the regions identified. We next tested whether activation patterns within these

potential source regions transcended the particular stopping domains. We used multi-voxel activation patterns to train a classifier to discriminate stopping from going in one modality (e.g., action stopping), to test whether it could identify stopping in the other modality (e.g. thought suppression). Finally, to examine behavioural relevance, we related inhibitory activations within these meta-analytic conjunction areas to individual variation in inhibition ability (e.g., suppression-induced forgetting and stop-signal reaction time) using behavioural partial least squares and multi-voxel pattern analysis. Any regions surviving these constraints was considered a strong candidate for a hub of inhibitory control. We hypothesized that these analyses would identify the right anterior DLPFC (Anderson & Hul-

1 bert, 2021; Benoit & Anderson, 2012; Depue et al., 2016;  
2 Guo et al., 2018), and right VLPFC (Aron et al., 2004;  
3 Levy & Wagner, 2011).

4 To verify that inhibitory control targets goal-relevant  
5 brain regions, we next confirmed that *a priori* target sites  
6 are suppressed in a goal-specific manner. Specifically, stop-  
7 ping retrieval should down-regulate hippocampal activity  
8 (Anderson et al., 2004; Benoit & Anderson, 2012; Depue  
9 et al., 2007; Gagnepain et al., 2014; Gagnepain et al.,  
10 2017; Levy & Anderson, 2012; Mary et al., 2020), more  
11 than does action stopping. In contrast, stopping actions  
12 should inhibit motor cortex more than does thought stop-  
13 ping (Schmitz et al., 2017). To determine whether these  
14 differences in modulation arise from inhibitory targeting  
15 by our putative domain-general prefrontal control regions,  
16 we used dynamic causal modelling (Friston et al., 2003).  
17 If both DLPFC and VLPFC are involved, as prior work sug-  
18 gests, we sought to evaluate whether one or both of these  
19 regions are critical sources of inhibitory control.

## 20 Results

### 21 The ability to inhibit unwanted thoughts is related to 22 action stopping efficiency

23 We first tested whether action stopping efficiency was  
24 associated to successful thought suppression. To quan-  
25 tify action stopping efficiency, we computed stop-signal  
26 reaction times (SSRTs) using the consensus standard inte-  
27 gration method (Verbruggen et al., 2019). We confirmed  
28 that the probability of responding to Stop trials ( $M = 0.49$ ,  
29  $SD = 0.07$ ; ranging from 0.36 to 0.69) fell within  
30 the recommended range for reliable estimation of SSRTs  
31 (Verbruggen et al., 2019), and that the probability of Go  
32 omissions ( $M = 0.002$ ,  $SD = 0.01$ ) and choice errors on  
33 Go trials ( $M = 0.04$ ,  $SD = 0.02$ ) were low. We next veri-  
34 fied that the correct Go RT ( $M = 600.91$  ms,  $SD = 54.63$   
35 ms) exceeded the failed Stop RT ( $M = 556.92$  ms,  $SD =$   
36 56.77) in all but one participant (9 ms difference between  
37 the failed Stop RT and correct Go RT; including this par-  
38 ticipant makes little difference to any analysis, so they  
39 were not excluded). Given that the integration method  
40 requirements were met, the average SSRT, our measure of  
41 interest, was 348.34 ms ( $SD = 51.25$  ms), with an average  
42 SSD of 230 ms ( $SD = 35.68$  ms).

43 We next verified that our Think/No-Think task had in-  
44 duced forgetting of suppressed items. We compared final  
100 recall of No-Think items to that of Baseline items that  
45 had neither been suppressed nor retrieved (see Meth-  
101 od). Consistent with a previous analysis of these data  
46 (Schmitz et al., 2017) and with prior findings (Anderson  
102 & Green, 2001; Anderson & Huddleston, 2012; Ander-  
103 son et al., 2004; Levy & Anderson, 2012), suppressing  
104 retrieval impaired No-Think recall ( $M = 72\%$ ,  $SD = 9\%$ )  
105 relative to Baseline recall ( $M = 77\%$ ,  $SD = 9\%$ ), yielding  
106 a suppression-induced forgetting (SIF) effect (Baseline –  
107 No-Think = 5%,  $SD = 9\%$ , one-tailed  $t_{23} = 2.55$ ,  $p =$   
108 0.009,  $d = 0.521$ ). Thus, suppressing retrieval yielded the  
109 predicted inhibitory aftereffects on unwanted thoughts.

110 To test the relationship between thought suppression  
111 and action stopping, we calculated a SIF score for each  
112 participant by subtracting No-Think from Baseline recall  
113 performance (Baseline – No-Think). This metric indexes  
114 the efficiency with which each participant could down-  
115 regulate later accessibility of suppressed items, an afteref-  
116 fect of suppression believed to be sensitive to inhibitory  
117 control (Anderson & Green, 2001). We then correlated the  
118 SSRT and SIF scores (excluding one bi-variate outlier; see  
119 Methods). Consistent with a potential shared inhibition  
120 process, better action stopping efficiency (faster SSRTs)  
121 was associated with greater SIF ( $r_{ss} = -0.492$ ,  $p = 0.014$ ,  
122 see Figure 4a; A detailed report of behavioural results is  
123 available in the supplementary analysis notebook).

124 Although we quantified SSRT with the integration  
125 method, this method may, at times, overestimate SSRTs  
126 because it does not consider times when participants fail  
127 to trigger the stopping process, known as trigger failures  
128 (Matzke et al., 2017). Trigger failures may arise, for exam-  
129 ple, when a participant is inattentive and misses a stop sig-  
130 nal. We recomputed SSRTs using a method that estimates  
131 trigger failure rate and that corrects SSRTs for these events  
132 (Matzke et al., 2017; Matzke et al., 2013). This method  
133 yielded shorter SSRTs ( $M = 278.84$  ms,  $SD = 41.13$  ms)  
134 than the integration method ( $M = 348.34$  ms), but did  
135 not alter the relationship between stopping efficiency and  
136 SIF ( $r = -0.383$ ,  $p = 0.065$ ), which remained similar to  
137 the relationship observed with integration method ( $r_{ss} =$   
138  $-0.492$ ,  $p = 0.014$ ). This alternate SSRT measure also  
139 did not qualitatively alter brain-behaviour relationships  
140 reported throughout. These findings suggest that atten-  
141 tional factors that generate trigger failures are unlikely  
142 to explain the relationship between thought and action  
143 inhibition.

### 144 Stopping actions and memories engages both right 145 DLPFC and VLPFC

146 We next isolated brain regions that could provide a source  
147 of inhibitory control over action and thought. The whole-  
148 brain voxel-wise conjunction analysis of the Stop > Go  
149 and the No-Think > Think contrasts revealed that both mo-  
150 tor and thought inhibition evoked conjoint activations in  
151 the right prefrontal cortex (PFC), specifically, the rDLPFC  
152 (middle frontal and superior frontal gyri), rVLPFC (ventral  
153 aspects of inferior frontal gyrus, including BA44/45, ex-  
154 tends into insula), precentral gyrus, and supplementary  
155 motor area (see Table 1a and Figure 3). These findings  
156 suggest a role of the right PFC in multiple domains of  
157 inhibitory control (Aron et al., 2004; Depue et al., 2016;  
158 Garavan et al., 1999), a key attribute necessary to establish  
159 dynamic targeting.

160 The observation that rDLPFC contributes to inhibitory  
161 control might seem surprising, given the published em-  
162 phasis on the rVLPFC in motor inhibition studies (Aron  
163 et al., 2004, 2014). It could be that rDLPFC activation  
164 arises from the need to alternate between the Stop-signal  
165 and Think/No-Think tasks, or from carryover effects be-  
166 tween tasks. We therefore compared the activations ob-

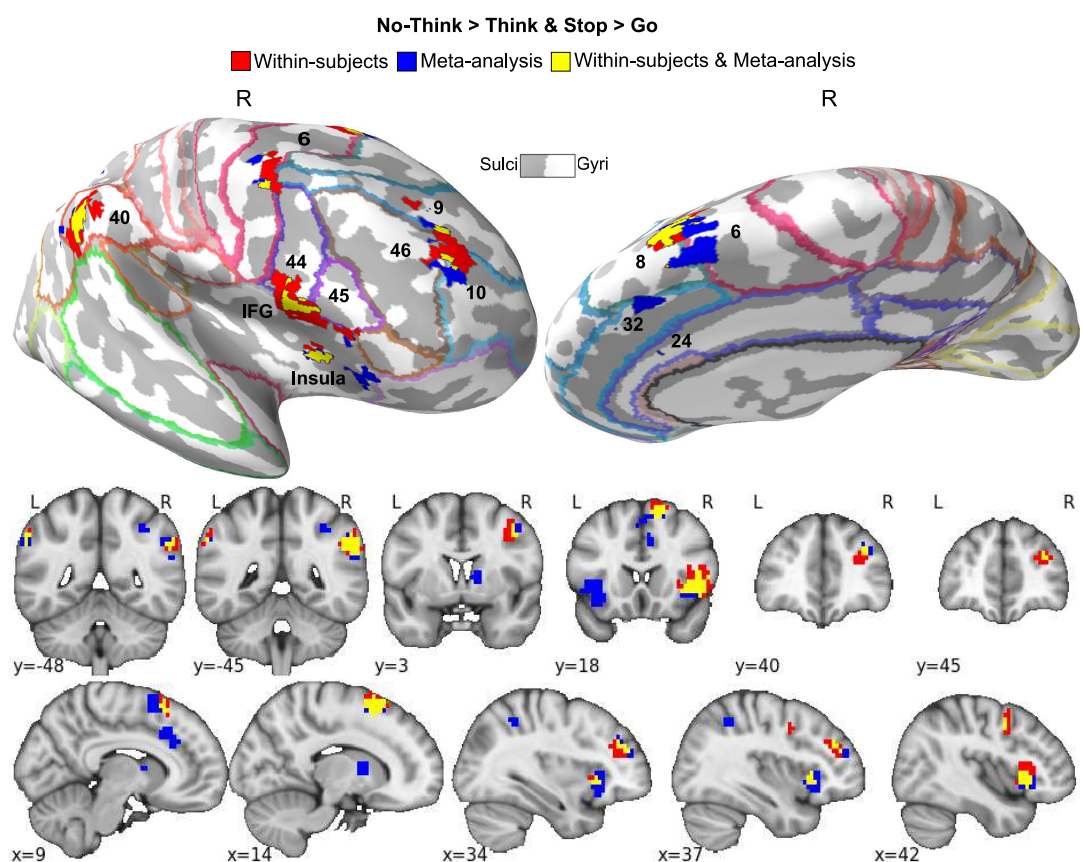


**Figure 3. Domain-general inhibition-induced activations.** Red: within-subjects ( $N = 24$ ) conjunction of the Stop > Go and the No-Think > Think contrasts thresholded at  $p < 0.05$  FDR corrected for whole-brain multiple comparisons. Blue: meta-analytic conjunction of Stop > Go and the No-Think > Think contrasts from independent 40 Stop-signal and 16 Think/No-Think studies. Yellow: overlap of the within-subjects and meta-analytic conjunctions. Results are displayed on an inflated MNI-152 surface with outlined and numbered Brodmann areas (top panel), as well as on MNI-152 volume slices (bottom panel). The brain images were generated using FreeSurfer software (<http://surfer.nmr.mgh.harvard.edu>), and PySurfer (<https://pysurfer.github.io>) and Nilearn (<https://nilearn.github.io>) Python (Python Software Foundation, DE, USA) packages.

served in our within-subjects conjunction analysis to a 24 meta-analytic conjunction analysis of independent Stop- 25 signal ( $N = 40$ ) and Think/No-Think ( $N = 16$ ) studies 26 (see Methods) conducted in many different laboratories 27 with different variations on the two procedures (see Guo 28 et al., 2018) for an earlier version with fewer studies). 29 The meta-analytic conjunction results were highly simi- 30 lar to our within-subjects results, with conjoint clusters 31 in matched regions of DLPFC, VLPFC (BA44/45, extend- 32 ing into insula), right anterior cingulate cortex, and right 33 basal ganglia (see Table 1b&c and Figure 3). Notably, in 34 both the within-subjects and meta-analytic conjunctions, 35 the domain-general activation in rDLPFC did not spread 36 throughout the entire right middle frontal gyrus but was 37 confined to the anterior portion of the rDLPFC, spanning 38 BA9/46 and BA10. The convergence of these conjunc- 39 tion analyses suggests that the involvement of the rDLPFC, 40 and our findings of conjoint activations across the two 41 inhibitory domains more broadly, do not arise from the 42 specific procedures of the inhibition tasks or to carryover 43 effects arising from our within-subjects design; rather, they 44 indicate a pattern that converges across laboratories and 45 different experimental procedures. 46

The domain-general stopping activations included areas outside of the prefrontal cortex (see Table 1a and Figure 3). We characterised these activations in relation to large-scale brain networks, using a publicly available Cole-Anticevic brain-wide network partition (CAB-NP) (Ji et al., 2019). We used the Connectome Workbench software (Marcus et al., 2011) to overlay our activations over the CAB-NP to estimate the parcel and network locations of our clusters. Domain-general clusters primarily were located in the Cingulo-Opercular (CON) and Frontoparietal (FPN) networks (86% of parcels fell within these two networks in the within-subjects conjunction), but also included Posterior-Multimodal and Language networks parcels (see Table S1 and Figure S1). Of the 21 cortical parcels identified for the within-subjects conjunction (see Table S1), the majority (57%) participated in the CON, whereas 29% were involved in the FPN; the independent meta-analysis yielded similar findings (56% vs 30%; see Table S2 and Figure S2). Our main right prefrontal regions both fea- 47 tured parcels from the CON; however, whereas rDLPFC was located solely in the CON (in both the within-subjects and meta-analytic conjunctions), the rVLPFC region also included parcels from the FPN.

**Table 1.** Within-subjects and meta-analysis domain-general inhibition-induced activations (Stop > Go & No-Think > Think)

Nr.	Hemisphere	Region	~BA	Network	MNI of the peak			Volume (mm <sup>3</sup> )
					x	y	z	
<i>a. Within-subjects, Stop &gt; Go &amp; No-Think &gt; Think</i>								
1	Right	Inferior frontal gyrus (VLPFC) Insula	44, 45	CON, FPN	45	18	8	5366
2	Right	Inferior parietal lobule	40	CON, FPN, PMM	63	-42	41	3611
3	Right	Supplementary motor area	6, 8	CON, FPN, LAN	15	18	64	2498
4	Right	Middle frontal gyrus (DLPFC) Superior frontal gyrus (DLPFC)	9, 10, 46	CON	33	42	23	1654
5	Right	Precentral gyrus	6	CON, FPN, LAN	42	3	41	945
6	Left	Inferior parietal lobule	40	CON, FPN	-60	-48	41	641
<i>b. Meta-analysis, Stop &gt; Go &amp; No-Think &gt; Think</i>								
1	Right	Inferior frontal gyrus (VLPFC) Insula	44, 45	CON, FPN	36	26	0	4523
2	Right/Left	Supplementary motor area	6, 8	CON, FPN, LAN	14	14	60	3071
3	Left	Inferior frontal gyrus Insula	44, 45	CON, FPN	-44	18	0	2970
4	Right	Inferior parietal lobule	40	CON, FPN, PMM	58	-46	34	2633
5	Right	Anterior cingulate cortex	24, 32	CON, FPN	6	22	38	1620
6	Right	Middle frontal gyrus (DLPFC) Superior frontal gyrus (DLPFC)	9, 10, 46	CON	36	50	22	844
7	Right	Basal ganglia			16	8	8	776
8	Left	Inferior parietal lobule	40	CON, FPN	-60	-50	34	608
9	Right	Precentral gyrus	6	CON, LAN	44	2	46	270
10	Right	Superior parietal lobule	7	FPN, DAN	34	-48	46	176
<i>c. Within-subjects &amp; Meta-analysis, Stop &gt; Go &amp; No-Think &gt; Think</i>								
1	Right	Inferior frontal gyrus (VLPFC) Insula	44, 45	CON, FPN	45	18	8	2666
2	Right	Inferior parietal lobule	40	CON, FPN, PMM	63	-42	38	1620
3	Right	Supplementary motor area	6, 8	CON, FPN, LAN	15	18	64	1418
4	Right	Middle frontal gyrus (DLPFC)	9, 10, 46	CON	33	39	26	338
5	Left	Inferior parietal lobule	40	CON, FPN	-60	-48	41	270
6	Right	Precentral gyrus	6	CON, LAN	42	3	41	135

1 Together, these findings confirm the role of both the  
 2 right anterior DLPFC and rVLPFC for both motor and mem-  
 3 ory inhibition. Moreover, they show that inhibitory control  
 4 recruits a larger network of regions, dominated by the  
 5 CON, and to a lesser degree, FPN. These findings suggest  
 6 that domain-general inhibitory control may reflect a spe-  
 7 cial configuration of the CON that includes elements of the  
 8 FPN and other networks. Notably, key regions of the FPN  
 9 were absent from all analyses, including the large middle  
 10 frontal region often taken as a hallmark of domain-general  
 11 cognitive control (Cole et al., 2013; Duncan, 2010).

12 **Right DLPFC and VLPFC support a common process  
 13 underlying suppression-induced forgetting and  
 14 action stopping efficiency**

15 We next examined whether action inhibition and thought  
 16 suppression depend on activity in the putative domain-  
 17 general regions identified in our meta-analytic conjunc-  
 18 tion analysis. We tested whether activation in the very  
 19 same voxels would predict SIF and SSRT. This test used  
 20 behavioural PLS analysis (see Methods), excluding one  
 21 behavioural bi-variate outlier from this analysis (see Meth-  
 22 ods), although the results with the outlier included did  
 23 not qualitatively differ.

24 The first latent variable (LV) identified by PLS accounted  
 25 for 78% of the covariance between inhibitory control ac-  
 26 tivations and behavioural measures of SSRT and SIF. To

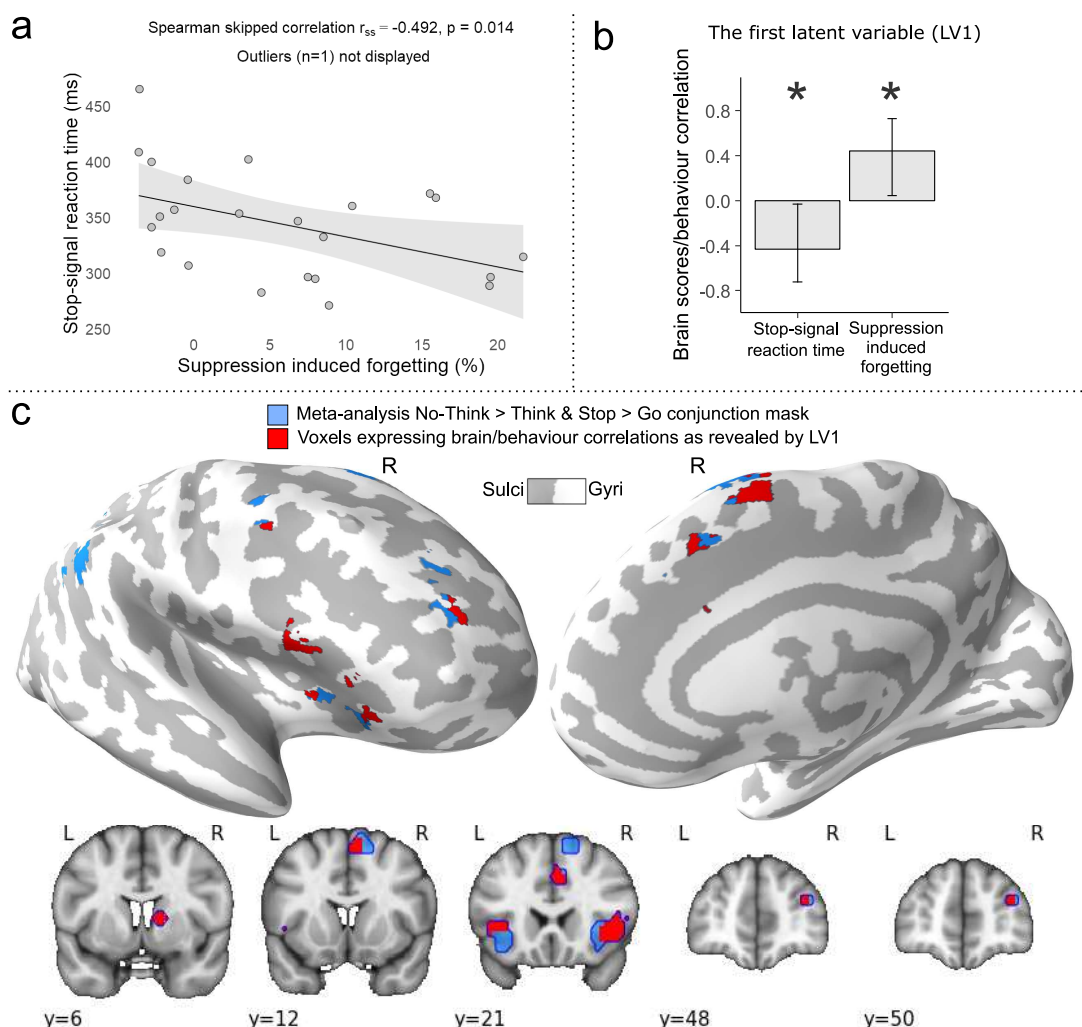


**Figure 4. Domain-general behavioural and brain/behaviour relationships.** (a) Better action stopping efficiency (shorter stop-signal reaction time) was associated with better inhibitory control over thoughts (percentage of items forgotten for No-Think relative to Baseline conditions at the final recall phase, i.e. suppression-induced forgetting;  $r_{ss} = -.492$ ,  $p = .014$ ). One bivariate outlier is not displayed on the scatterplot. Shading represents 95% CI. (b and c) A behavioural partial least squares (PLS) analysis was conducted to identify brain areas where individual variation in inhibition ability (SSRT and SIF) was related to increased inhibition-induced activity (main effect contrast of inhibition from the within-subject experiment, masked by the meta-analytic conjunction). (b) The first latent variable (LV1) identified voxels showing a significant pattern of brain/behaviour correlations to both SSRT and SIF (error bars indicate bootstrapped 95% CI). (c) The voxel salience map expressing LV1. Blue: meta-analytic conjunction mask. Red: voxels showing a significant pattern of brain/behaviour correlations as revealed by the LV1; thresholded at bootstrapped standard ratio 1.96, corresponding to  $p < 0.05$ , two-tailed. Results are displayed on an inflated MNI-152 surface (top panel), as well as on MNI-152 volume slices (bottom panel). The brain images were generated using FreeSurfer software (<http://surfer.nmr.mgh.harvard.edu>), and PySurfer (<https://pysurfer.github.io>) and NiLearn (<https://nilearn.github.io>) Python (Python Software Foundation, DE, USA) packages.

1 specify how brain activation relates to those measures, we 15  
2 computed voxel saliences and a brain score for each par- 16  
3 ticipant (see Methods). A brain score indicates how much 17  
4 a participant expresses the multivariate spatial pattern of 18  
5 correlation between inhibitory control brain activations 19  
6 and behavioural measures of action and memory control 20  
7 captured by a LV. Thus, correlations between brain scores 21  
8 and behavioural measurements identify the direction and 22  
9 the strength of the relationship captured by a LV (i.e., the 23  
10 corresponding voxel salience over that LV). Within our 24  
11 meta-analytic conjunction regions (see Methods; Table 1b, 25  
12 Figure 3 and Figure 4c), participants' brain scores for the 26  
13 first LV correlated negatively with SSRT scores ( $r = -0.432$ , 27  
14 [-0.724, -0.030] bootstrapped 95% CI) and positively with 28

SIF scores ( $r = 0.441$ , [0.044, 0.729] bootstrapped 95% CI; Figure 4b). In other words, for voxels with high positive salience for this LV, a higher BOLD signal for the Inhibit > Respond contrast predicted faster SSRTs (i.e., better action stopping speed) and larger amounts of SIF (i.e., better memory inhibition). Voxels associated with significant positive salience arose across the entire set of domain-general conjunction regions except for the inferior parietal lobules (see Table 2 and Figure 4c). No voxels were associated with a significant negative salience (i.e., the opposite pattern).

These findings support the hypothesis that the stopping-evoked activity identified in our conjunction analyses plays behaviourally important roles both in stopping actions

**Table 2.** Control network regions showing a significant pattern of brain/behaviour correlations as revealed by the first latent variable of the PLS analysis.

Brain region	~BA	MNI of the peak			Volume (mm <sup>3</sup> )	
		x	y	z		
Right	Inferior frontal gyrus (VLPFC) Insula	44, 45	45	21	0	3375
Right	Anterior cingulate cortex	24, 32	6	30	34	1418
Left	Inferior frontal gyrus Insula	44, 45	-33	21	4	1046
Right/Left	Supplementary motor area	6, 8	6	9	64	1013
Right	Basal ganglia		15	3	8	709
Right	Middle frontal gyrus (DLPFC)	10, 46	33	48	19	304
Right	Precentral gyrus	6	42	3	41	68

1 efficiently and in forgetting unwanted thoughts, a key 41  
2 attribute necessary to establish dynamic targeting. 42

### 3 Stopping actions and stopping thoughts 43 4 downregulates domain-specific target areas 44

5 A key attribute of dynamic targeting is that the domain- 45  
6 specific target areas are inhibited in response to activity of 46  
7 the domain-general source of inhibitory control, when the 47  
8 specific task goals require it. For example, inhibiting motor 48  
9 responses downregulates activity in M1 (Badry et al., 49  
10 2009; Chowdhury et al., 2019; Mattia et al., 2012; Sumi- 50  
11 tash et al., 2019; Zandbelt & Vink, 2010), whereas inhibiting 51  
12 memory retrieval downregulates activity in the hippocampus 52  
13 (Anderson et al., 2016; Anderson & Hanslmayr, 53  
14 2014; Anderson et al., 2004; Benoit & Anderson, 2012; 54  
15 Benoit et al., 2016; Benoit et al., 2015; Depue et al., 2007; 55  
16 Gagnepain et al., 2017; Hu et al., 2017; Levy & Anderson, 56  
17 2012; Liu et al., 2016). Previously, we reported both of 57  
18 the foregoing patterns in a separate analysis of the current 58  
19 data (Schmitz et al., 2017). In the analyses below, we 59  
20 reconfirmed these findings using the left M1 and the right 60  
21 hippocampus ROIs which we defined specifically for the 61  
22 current DCM analyses (see Methods). 62

23 Dynamic targeting predicts a crossover interaction such 63  
24 that action stopping suppresses M1 more than it does the 64  
25 hippocampus, whereas thought stopping should do the re- 65  
26 verse. A repeated-measures analysis of variance (ANOVA) 66  
27 confirmed a significant interaction between modulatory 67  
28 target regions (M1 vs. hippocampus) and stopping modal- 68  
29 ity (stopping actions vs. stopping thoughts) on the BOLD 69  
30 signal difference between the respective inhibition and 70  
31 non-inhibition conditions in each modality ( $F_{1,23} = 42.71$ , 71  
32  $p < 0.001$ ; Figure 5a). Whereas stopping motor responses 72  
33 (Stop - Go) evoked greater downregulation of the M1 than 73  
34 the hippocampus ROI ( $t_{23} = 5.89$ ,  $p < 0.001$ ,  $d = 1.202$ ), 74  
35 suppressing thoughts (No-Think - Think) evoked larger 75  
36 downregulation of the hippocampus than the M1 ROI ( $t_{23} = 76$   
37  $= 3.22$ ,  $p = 0.004$ ,  $d = 0.658$ ). Thus, action stopping 77  
38 and thought suppression preferentially modulated the left 78  
39 M1 and right hippocampus, respectively. Critically, these 79  
40 modulations were not solely produced by up-regulation 80

in the Go or Think conditions, as illustrated by negative BOLD response during Stop ( $t_{23} = -3.88$ ,  $p < 0.001$ ,  $d = 0.791$ ) and No-Think ( $t_{23} = -1.84$ ,  $p = 0.04$ ,  $d = 0.375$ ) conditions (see Figure 5b). Thus, brain regions involved in representing the type of content requiring inhibition for each stopping task showed evidence of interrupted function during stopping, consistent with the requirements of dynamic targeting.

### Action and thought stopping share common representations in the right DLPFC and VLPFC, but not in targeted regions

It is possible that despite the shared locus of activation in the rDLPFC and rVLPFC, the pattern of activation across voxels within these regions may fundamentally differ for action and thought stopping, a possibility that cannot be excluded with conventional univariate methods. However, dynamic targeting predicts similarities in the multivariate pattern of inhibitory control activity across voxels in the two tasks. Similarities should arise because of the shared engagement of a modality independent stopping process, even if some differences arise because of the stimulus processing and output pathways uniquely required to be each stopping process. To identify the similarities, we trained a classifier on the difference between Inhibit and Respond conditions in one modality and tested the ability to classify Inhibit and Respond conditions in the other domain. Such cross-modality decoding should not be possible in domain-specific target regions, reflecting their specialised involvement in action or memory stopping.

We performed the classification analysis on the rDLPFC, rVLPFC, right hippocampus, and left M1 ROIs which we defined for our DCM analyses (see Methods). The cross-modality classification revealed that a classifier trained on one modality could discriminate Inhibition from Respond conditions in the other modality significantly above chance (50%) for both rDLPFC ( $M = 57\%$ ,  $SD = 10\%$ , one-tailed  $t_{23} = 3.48$ ,  $p = 0.004$ ,  $d = 0.711$ ) and rVLPFC ( $M = 60\%$ ,  $SD = 12\%$ , one-tailed  $t_{23} = 3.93$ ,  $p = 0.001$ ,  $d = 0.802$ ). This cross-task decoding suggests a domain-general inhibitory control process in these regions (see

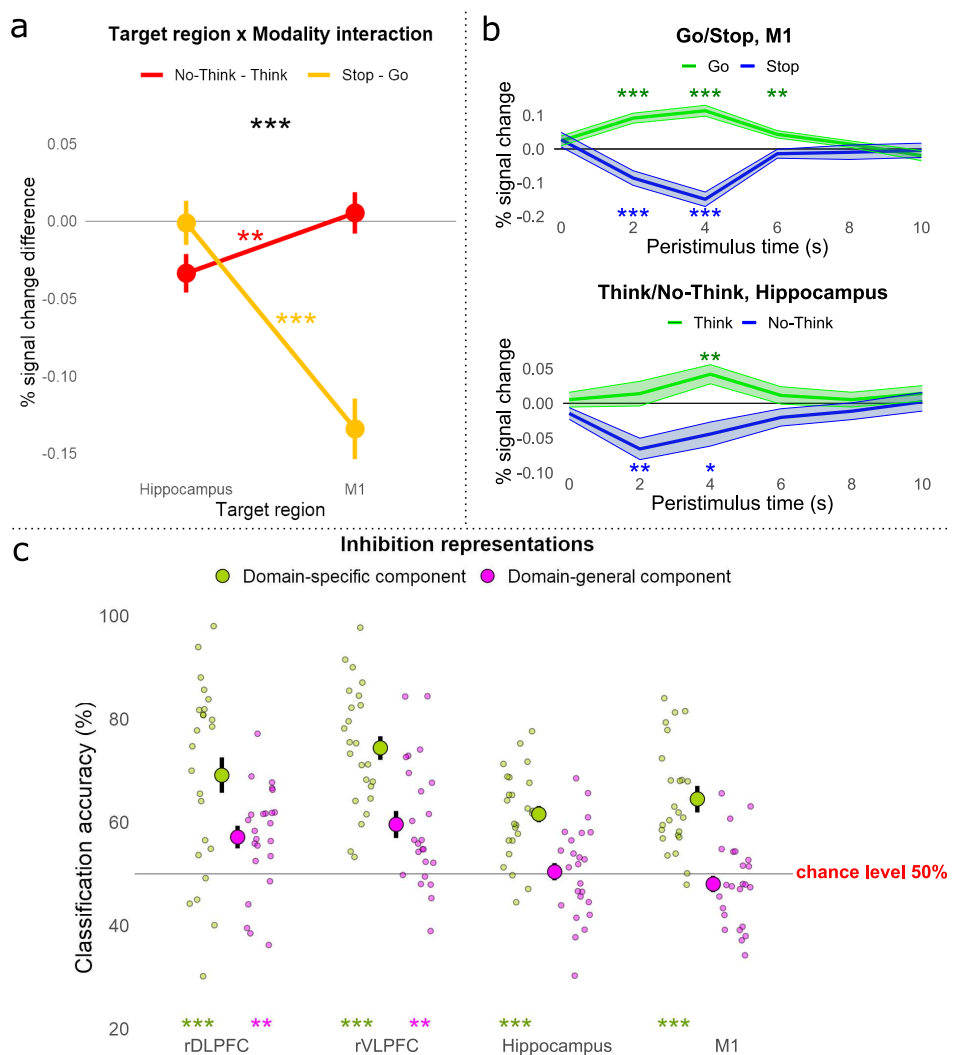


**Figure 5. ROI analysis of domain-specific and domain-general modulation during thought and action suppression.** \*\*\* $p < 0.001$ ; \*\* $p < 0.01$ ; \* $p < 0.05$ . Error bars represent within-subject standard error. (a) Target areas M1 and hippocampus were modulated in a domain-specific manner. We calculated the BOLD signal in each target ROI for each condition by averaging across the time points from 2 to 8 s post-stimulus onset and subtracting out the onset value to account for pretrial variability. Then we subtracted the values of Go from Stop and Think from No-Think and entered them into a region by modality repeated-measures ANOVA. The ANOVA confirmed a significant interaction between modulatory target regions and stopping modality. Stopping actions (in yellow) evoked greater downregulation of M1 than of the hippocampus but suppressing thoughts (in red) evoked greater downregulation of the hippocampus than of M1. (b) The BOLD signal time-course in M1 (top panel) and hippocampus (bottom panel). During inhibition conditions (Stop and No-Think; in blue), the BOLD signal decreased below the baseline, whereas during respond conditions (Go and Think; in green) the BOLD signal increased above the baseline. (c) Using MVPA, we tested whether action and thought inhibition share a common voxel activation pattern within the four ROIs. We performed two types of pattern classification to identify domain-general (cross-task classification; in violet) and domain-specific (between-task classification; in green) components within each ROI. Large circles represent group average classification accuracies, and small circles represent individual participant accuracies.

Figure 5c). We also sought to identify differences in the patterns of activation across tasks by training a classifier to discriminate Stop from No-Think trials (see Methods). We found a significant domain-specific component in both rDLPFC ( $M = 69\%$ ,  $SD = 18\%$ , one-tailed  $t_{23} = 5.09$ ,  $p < 0.001$ ,  $d = 1.039$ ) and rVLPFC ( $M = 74\%$ ,  $SD = 12\%$ ,  $t_{23} = 10.10$ ,  $p < 0.001$ ,  $d = 2.06$ ).

In contrast to the patterns observed in the prefrontal cortex, we observed no evidence of cross-task decoding in the modality-specific regions targeted by inhibitory control. This pattern arose for both right hippocampus ( $M = 50\%$ ,  $SD = 9\%$ , one-tailed  $t_{23} = 0.23$ ,  $p = 1$ ,  $d = 0.046$ )

and also left M1 ( $M = 48\%$ ,  $SD = 8\%$ , one-tailed  $t_{23} = -1.15$ ,  $p = 1$ ,  $d = -0.235$ ), in which the cross-modality classifier accuracy did not significantly differ from chance performance (see Figure 5c). Nevertheless, these putative target regions responded very differently to the two modalities of inhibitory control, as evidenced by presence of significant domain-specific information in each region. A classifier could reliably distinguish No-Think trials from Stop trials within both the right hippocampus ( $M = 62\%$ ,  $SD = 9\%$ ,  $t_{23} = 6.59$ ,  $p < 0.001$ ,  $d = 1.346$ ) and left M1 ( $M = 65\%$ ,  $SD = 10\%$ ,  $t_{23} = 6.85$ ,  $p < 0.001$ ,  $d = 1.399$ ; see Figure 5c).

Because we z-normalised activation within each of these regions within each task, the ability to distinguish No-Think from Stop trials was not based on differences in overall univariate signal, but instead on information contained in distinct patterns of activity in each task. These findings reinforce the assumption that the hippocampus and M1 are uniquely affected by thought and action stopping respectively, as expected for domain-specific targets of inhibitory control. Taken together, these contrasting findings from the PFC and domain-specific regions are compatible with the view that rDLPFC and rVLPFC jointly contribute to a domain-general stopping process that dynamically targets different regions, depending on the nature of the content to be suppressed.

### Adaptive forgetting can be predicted using action stopping representations

Because dynamic targeting posits that LPFC contains domain-general stopping representations, training a classifier to distinguish stopping in one domain should predict stopping behaviour in other domains. For example, the ability of an action stopping classifier to distinguish when people are suppressing thoughts raises the intriguing possibility that it also may identify participants who successfully forget those thoughts. To test this possibility, we capitalised on an active forgetting phenomenon known as the conflict reduction benefit (for a review, see [Anderson and Hulbert, 2021](#)). The conflict-reduction benefit refers to the declining need to expend inhibitory control resources that arises when people repeatedly suppress the same intrusive thoughts. This benefit arises because inhibitory control induces forgetting of inhibited items, which thereafter cause fewer control problems. For example, over repeated inhibition trials, activation in rDLPFC, rVLPFC, and anterior cingulate cortex decline, with larger declines in participants who forget more of the memories they suppressed ([Anderson & Hulbert, 2021](#); [Kuhl et al., 2007](#); [Wimber et al., 2015](#)). If an action stopping classifier detects the inhibition process, two findings related to conflict-reduction benefits should emerge. First, over Think/No-Think task blocks, the action-stopping classifier should discriminate thought suppression less well, with high classification in early blocks that drops as memories are inhibited. Second, this decline should be larger for people showing greater SIF.

We examined how accurately an action stopping classifier distinguishes No-Think from Think conditions for the 8 fMRI runs. The rDLPFC showed a robust linear decline ( $F_{7,157} = 11.19$ ,  $p = 0.001$ ) in classification accuracy from the first ( $M = 77\%$ ) to the eighth ( $M = 40\%$ ) run, consistent with a conflict-reduction benefit (see Figure S4A). The rVLPFC exhibited a marginal linear decline ( $F_{1,157} = 3.04$ ,  $p = 0.083$ ) in classification accuracy from the first ( $M = 64\%$ ) to the eighth ( $M = 32\%$ ) run (see Figure S5A). Critically, for both rDLPFC ( $r_{ss} = -0.618$ ,  $p = 0.001$ ; Figure S4B) and rVLPFC ( $r_{ss} = -0.682$ ,  $p < 0.001$ ; Figure S5B), participants showing greater SIF exhibited a steeper classification accuracy decline. This suggests that adaptive

forgetting had diminished demands on inhibitory control. Consistent with the involvement of inhibition, the decline in classifier performance also was associated to SSRT for both rDLPFC ( $r = 0.525$ ,  $p = 0.008$ ; Figure S4C) and rVLPFC ( $r_{ss} = 0.590$ ,  $p = 0.002$ ; Figure S5C). These findings support the view that suppressing unwanted thoughts engages a domain-general inhibition process indexed by action stopping and suggests that both rDLPFC and rVLPFC support this process.

### Right DLPFC and VLPFC dynamically couple with their domain-specific target areas to down-regulate their activity

Although rDLPFC and rVLPFC contribute to action and thought stopping, it remains to be shown whether either or both regions causally modulate target regions during each task, one of the five key attributes of dynamic targeting. On the one hand, rVLPFC alone might show dynamic targeting, exerting inhibitory modulation on the hippocampus or M1 in a task-dependent manner, as emphasized in research on motor response inhibition ([Aron et al., 2004, 2014](#)); rDLPFC may only be involved to maintain the inhibition task set in working memory, possibly exerting a modulatory influence on rVLPFC to achieve this (rVLPFC alone model). On the other hand, rDLPFC alone might show dynamic inhibitory targeting, consistent with the emphasis on the rDLPFC as the primary source of inhibitory control in research on thought suppression ([Anderson & Hanslmayr, 2014](#); [Anderson & Hulbert, 2021](#)); rVLPFC may only be involved when attention is captured by salient stimuli, such as the stop signal or intrusions, possibly exerting a modulatory effect on rDLPFC to upregulate its activity (rDLPFC alone model). A third possibility is that rDLPFC and rVLPFC each contribute to top-down modulation in a content-specific manner, with only rDLPFC modulating the hippocampus during memory control, but only rVLPFC modulating M1 during action stopping. By this independent pathway hypothesis, both structures are pivotal to inhibitory control functions, but only with respect to their special domains, contrary to dynamic targeting. Finally, both rDLPFC and rVLPFC may be involved in dynamic targeting, modulating both hippocampus and M1 in a task-dependent manner; they may interact with one another to support stopping (Parallel modulation hypothesis).

To determine the way that rDLPFC and rVLPFC interact with each other and with the target regions of inhibitory control (M1 and hippocampus) we analysed effective connectivity between regions using dynamic causal modelling (DCM, see Methods). DCM accommodates the polysynaptic mediation of the causal influence that prefrontal regions could exert on activity in the hippocampus and in M1 ([Anderson et al., 2016](#)). DCM is ideally suited to test our hypotheses about which prefrontal regions drive inhibitory interactions, whether these vary by task context, and whether and how those prefrontal regions interact with one another to achieve inhibitory control.

Our model space included a null model with no mod-

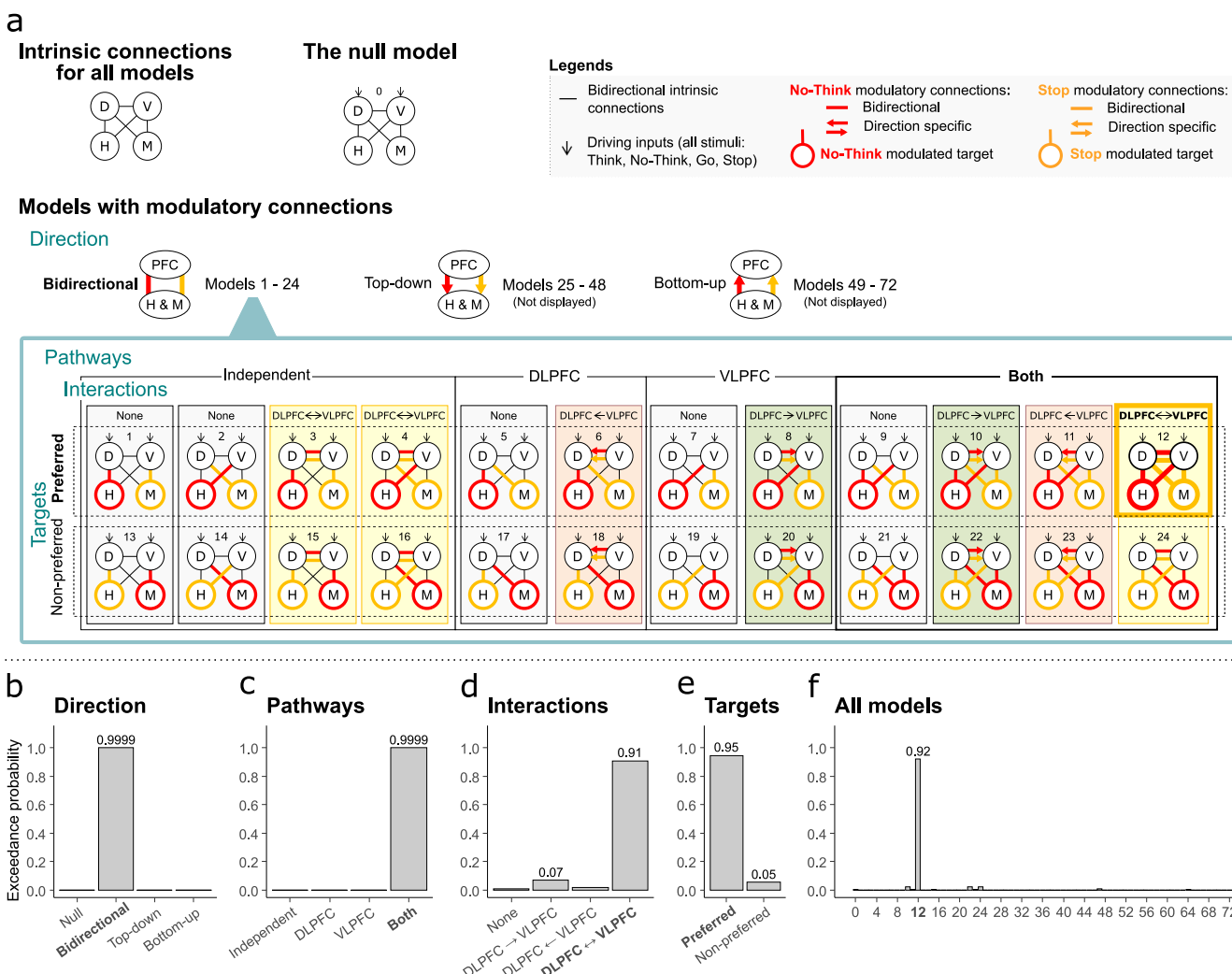


**Figure 6. DCM model space and results.** (a) DCM analysis determined the most likely inhibition-related interactions between domain-general inhibitory control source areas (D: rDLPFC, V: rVLPFC) and domain-specific target areas (H: right hippocampus, M: left M1). We compared 73 alternative models grouped into four family types. Direction: three families according to whether the source-target modulation is bidirectional, top-down, or bottom-up (we display only the 24 models within the bidirectional family as the further grouping was identical within each of the three families). Pathways: four families differing according to how Stop and No-Think modulate the pathways: independent modulation of target regions by rDLPFC and rVLPFC; rDLPFC only modulation; rVLPFC only modulation; or modulation by both rDLPFC and rVLPFC. Interactions: four families differing according to how Stop and No-Think modulate interactions between the rDLPFC and rVLPFC regions: no interactions; rVLPFC modulates rDLPFC; rDLPFC modulates rVLPFC; or bidirectional interaction between rDLPFC and rVLPFC. Targets: two families differing according to whether Stop and No-Think modulate the prefrontal connectivity with the preferred targets (M1 when stopping actions and hippocampus when stopping thoughts) or with the non-preferred targets (hippocampus when stopping actions and M1 when stopping thoughts). BMS (reporting exceedance probability to which a model is more likely to other models considered) overwhelmingly favoured models with (b) bidirectional source-target modulation; (c) both rDLPFC and rVLPFC modulating both the hippocampus and M1; (d) bidirectional interactions between the rDLPFC and rVLPFC; (e) the preferred target modulation. (f) The overall winning model also was strongly favoured by BMS even when directly assessing all 73 models, side by side, without grouping them into model families.

ulatory connections and 72 distinct modulatory models (see Figure 6a) differing according to whether the source-target modulation was bidirectional, top-down, or bottom-up, whether rDLPFC, rVLPFC or both were sources of modulation, whether rDLPFC and rVLPFC interacted during inhibition tasks, and whether the site on which top-down modulation acted was appropriate to the inhibition task or not. We first compared the null model and models in which the direction of source-target modulation was either bidirectional, top-down, or bottom-up (24 models in each of the three families). The findings from these

connectivity analyses were unambiguous. Bayesian Model Selection (BMS) overwhelmingly favoured models with bidirectional connections between the sources (rDLPFC and rVLPFC) and targets (M1 and hippocampus) with an exceedance probability (EP) of 0.9999. In contrast, the null modulation, top-down, and bottom-up models had EP of 0/0.0001/0, respectively (see Figure 6b). Exceedance probability refers to the extent to which a model is more likely in relation to other models considered. The bidirectional modulation confirms the existence of a top-down (our focus of interest) influence that prefrontal regions

1 exert on activity in the hippocampus and in M1, alongside 59  
2 bottom-up modulation. 60

3 We next compared, within the 24 bidirectional models 61 (models 1-24, see Figure 6a), whether either rDLPFC 62 or rVLPFC was the sole dominant top-down source of 63 inhibitory control (rDLPFC only vs rVLPFC only models) to 64 models in which both regions comprised independent mod- 65 ulatory pathways (independent pathways model) or in- 66 stead, contributed cooperatively to achieving top-down in- 67 hibitory control (parallel inhibition model). The BMS over- 68 whelmingly favoured models in which both rDLPFC and 69 rVLPFC contributed to modulating both the hippocampus 70 and M1 with an exceedance probability (EP) of 0.9999; 71 in contrast, Independent Pathways, rDLPFC alone, and 72 rVLPFC alone models had an EP of 0.0001/0/0, respec- 73 tively (see Figure 6c).

74 We next sought to distinguish subfamilies within this 75 parallel model (models 9-12, and 21-24, see Figure 6a) 76 that varied according to whether and how rDLPFC and 77 rVLPFC interacted during inhibition: No-interaction at all 78 between rDLPFC and rVLPFC (none); Unidirectional inter- 79 action from rVLPFC to rDLPFC (unidirectional rVLPFC); 80 Unidirectional interaction from rDLPFC to rVLPFC (unidi- 81 rectional rDLPFC) and bidirectional interaction (rDLPFC 82 and rVLPFC interact with each other). If rDLPFC and 83 rVLPFC work as a functional unit to achieve inhibitory con- 84 trol, one would expect clear evidence that some form of 85 interaction occurs. Consistent with this view, BMS strongly 86 favoured models with bidirectional interactions between 87 the rDLPFC and rVLPFC (EP = 0.91; EP for the none, 88 unidirectional rDLPFC, and unidirectional rVLPFC being 89 0.01/0.07/0.02; see Figure 6d).

90 Next, we tested whether inhibitory control is dynam- 91 ically targeted to the appropriate target structure (e.g., 92 hippocampus or M1), depending on which process needs 93 to be stopped (memory retrieval or action production). Ac- 94 cording to our hypothesis, the rDLPFC and rVLPFC should 95 down-regulate hippocampal activity during thought sup- 96 pression, but should instead modulate M1, during action 97 stopping. To test this dynamic targeting hypothesis, we 98 compared the two remaining models (12 and 24, see 99 Figure 6a) within our winning parallel/bidirectional sub- 100 family. In the “preferred targets” model, rDLPFC and 101 rVLPFC modulated the hippocampus during thought sup- 102 pression, but M1 during action stopping; in the “non- 103 preferred targets” model, these structures modulated 104 content-inappropriate targets (e.g. M1 during thought 105 suppression, but hippocampus during action stopping). 106 BMS strongly favoured the model with preferred (EP = 107 0.95) over the non-preferred (EP = 0.05) target modula- 108 tion (see Figure 6e). Indeed, the overall winning model 109 also was strongly favoured by BMS even when directly 110 assessing all 73 models, side by side, without grouping 111 them into model families and subfamilies (BMS = 0.92; 112 see Figure 6f).

113 The preferential modulations of hippocampus or M1, 114 depending on whether thoughts or actions are to be sup- 115 pressed, confirm our key hypothesis that top-down mod- 116

ulation by rDLPFC and rVLPFC is dynamically targeted 117 depending on participants’ task goals. Together, the re- 118 sults of the DCM analysis suggest that, when inhibiting a 119 prepotent response, the domain-general inhibitory control 120 regions, rDLPFC and rVLPFC, interact with each other and 121 are both selectively coupled with M1 when stopping ac- 122 tions and selectively coupled with the hippocampus when 123 stopping thoughts.

## Discussion

The current findings identify two regions within the right LPFC that possess a dynamic targeting capability supporting the inhibition of both unwanted motor actions and thoughts: anterior rDLPFC and rVLPFC. These regions exhibited the five attributes needed to infer dynamic targeting. Both are engaged by diverse domains of inhibitory control, a finding supported not only by a within-subject conjunction analysis, but also via a meta-analytical conjunction; both show evidence of cross-task decoding, indicating that the representations formed in these regions are sufficiently general so that they recur in highly different stopping domains. Both regions are relevant to individual variation in inhibitory efficiency in both action stopping and thought suppression. Indeed, the multivariate activation pattern for action stopping resembled that for thought suppression enough so that it could be used as a proxy to predict how successfully people had suppressed their thoughts. Both regions are engaged alongside significant down-regulations in domain-specific target regions that we predicted *a priori* likely would require top-down inhibition; and both prefrontal regions show top-down effective connectivity with M1 and hippocampus during action stopping and thought suppression, supporting a causal role in their down-regulation. Critically, effective connectivity from both rDLPFC and rVLPFC to these two target regions dynamically shifted as participants moved between action to thought stopping, as would be required of a domain-general mechanism that can be flexibly targeted to suppress specialised content in multiple domains.

Based on these and related findings, we propose that anterior rDLPFC and rVLPFC constitute key hubs for a domain-general inhibitory control mechanism that can be dynamically targeted at diverse content represented throughout the brain. We focused here on the stopping of simple manual actions and verbal thoughts. Given this approach, this study does not address the breadth of thought content that can be targeted by this mechanism. However, when considered alongside the growing literature on retrieval suppression, the breadth of content is considerable. For example, the anterior rDLPFC and rVLPFC regions identified in the meta-analytic conjunction have been observed during the suppression of a range of stimuli, including words (Anderson et al., 2004; Benoit & Anderson, 2012; Levy & Anderson, 2012), visual objects (Gagnepain et al., 2014; Mary et al., 2020), neutral and aversive scenes (Benoit et al., 2015; Depue et al., 2007; Gagnepain et al., 2017; Liu et al., 2016) and person-specific fears about the future (Benoit et al., 2016). In addition,

1 during retrieval suppression, these frontal regions exert 59  
2 top-down inhibitory modulation not only of the hippocam- 60  
3 pus (Anderson et al., 2016; Levy & Anderson, 2012), but 61  
4 also of other domain-specific content regions, including 62  
5 areas involved in representing visual objects (Gagnepain 63  
6 et al., 2014; Mary et al., 2020), places (Benoit et al., 64  
7 2015; Gagnepain et al., 2017), and also emotional content 65  
8 in the amygdala (Depue et al., 2007; Gagnepain et al., 66  
9 2017). Content-specific modulations are triggered espe- 67  
10 cially when these types of content intrude into awareness 68  
11 in response to a cue and need to be purged (Gagnepain 69  
12 et al., 2017), indicating that inhibition can be dynamically 70  
13 targeted to diverse cortical sites to meet control demands. 71  
14 The current findings broaden the scope of this mecha- 72  
15 nism further by showing that it is not limited to stopping 73  
16 retrieval processes, but also extends to stopping the prepa- 74  
17 ration and execution of motor responses, consistent with a 75  
18 broad mechanism involved in self-control over action and 76  
19 thought. 77

20 We considered the possibility that one of these two 78  
21 prefrontal regions is central to implementing top-down 79  
22 inhibitory control, with the other providing upstream in- 80  
23 puts essential to initiate successful inhibitory control. Our 81  
24 effective connectivity analysis probed alternative hypoth- 82  
25 eses about the way rDLPFC and rVLPFC interact during 83  
26 inhibitory control. RDLPFC might implement the true in- 84  
27 inhibitory signal, receiving salience detection input from 85  
28 rVLPFC that up-regulates rDLPFC function. Alternatively, 86  
29 rVLPFC may implement inhibition, with rDLPFC preserving 87  
30 task set by sending driving inputs to the rVLPFC. Our 88  
31 findings indicate that both structures contributed in parallel to 89  
32 top-down inhibitory control and interacted bidirectionally 90  
33 during both action and thought stopping. Little evidence 91  
34 suggested a strong asymmetry in how rDLPFC and rVLPFC 92  
35 interacted, as should arise if one region simply served a 93  
36 role in salience detection or task-set maintenance. These 94  
37 findings suggest that rDLPFC and rVLPFC act together to 95  
38 implement top-down inhibitory control. Although it might 96  
39 seem surprising that two spatially segregated prefrontal 97  
40 regions would act in concert to achieve this function, it 98  
41 seems less unusual considering their potential role in the 99  
42 Cingulo-Opercular network (CON). The majority of the 100  
43 regions identified in our inhibition conjunction analysis 101  
44 participate in this network, suggesting that it may play 102  
45 an important role in achieving inhibitory control. Given 103  
46 the strong integrated activity of this network, elements 104  
47 of which are distributed throughout the brain (Cocuzza 105  
48 et al., 2020; Cole et al., 2013), this suggests future work 106  
49 should examine how rDLPFC and rVLPFC work together 107  
50 with other elements of this network to achieve successful 108  
51 inhibitory control. 109

52 The current proposal contrasts with models that empha- 110  
53 sise the primacy of either rVLPFC or rDLPFC in inhibitory 111  
54 control, and which have not addressed dynamic targeting 112  
55 to diverse content. Research on motor inhibition has em- 113  
56 phasised the rVLPFC as the source of top-down inhibitory 114  
57 control (Aron et al., 2004, 2014), although without evi- 115  
58 dence to exclude the role of rDLPFC. Indeed, studies cited 116

as favouring the selective role of rVLPFC often support contributions of the anterior rDLPFC structure identified here. For example, whereas intracranial stimulation in primates establishes the causal necessity of the rVLPFC in motor stopping, so too does stimulation of the dorsal bank of the principal sulcus, the putative monkey homologue of the rDLPFC in humans (Sasaki et al., 1989); and whereas intracranial recordings in humans show stopping-related activity in rVLPFC, they also reveal it in anterior rDLPFC and often prior to rVLPFC (Swann et al., 2013). Research on thought suppression has emphasised the rDLPFC as the source of top-down inhibitory control (Anderson et al., 2016; Anderson & Hanslmayr, 2014; Anderson et al., 2004); but most studies supporting the role of rDLPFC in thought suppression also reveal activations in the rVLPFC (Guo et al., 2018). Indeed, as our within-subjects and meta-analytic conjunctions unambiguously confirm, both regions are recruited during both inhibitory control tasks. The current study goes further than establishing conjoint activation: Pattern classification and connectivity analyses show the involvement of both regions in the dynamics of control, without selectivity. These findings validate the importance of both regions, establish the domain-generality of their influence, and demonstrate the dynamic inhibitory targeting capacity necessary to infer a flexible control mechanism.

The present findings highlight a potentially important difference between the brain networks involved in inhibitory control and other forms of cognitive control that do not require the inhibition of a motor or cognitive process. Maintaining rules in working memory, implementing task sets, performing multi-tasking, and manipulating information actively are all clear cases of cognitive control that can require interference resolution, but do not necessarily entail active stopping. The above tasks engage the widely discussed fronto-parietal network (FPN), often assigned a central role in implementing cognitive control more broadly (Cole et al., 2013; Cole & Schneider, 2007; Duncan, 2010; Fox et al., 2005). One might assume that because inhibitory control is a form of cognitive control that the FPN would be central to it as well. Nevertheless, the FPN, though involved in our tasks, appeared less prominent than the CON, which accounted for the majority of distinct cortical parcels participating in our domain-general inhibition regions. We found little evidence for involvement of major areas of the FPN, including much of the middle frontal gyrus bilaterally in our multimodal inhibition regions. As our meta-analysis and within-subjects comparisons confirm, inhibitory control is strongly right lateralised, which also is not a feature emphasised in research on the FPN. Our findings raise the possibility that stopping actions and thoughts may rely on a distinct network, with different functional characteristics to the FPN.

Dynamic inhibitory targeting provides a neurocognitive framework that can account for both associations and dissociations in the abilities to suppress unwanted thoughts and actions. On the one hand, deficits in both action and

thought stopping should arise with dysfunction in the rDLPFC or rVLPFC, given the common reliance of these abilities on those regions. Such associations occur frequently. In the general population, people scoring highly on self-report measures of impulsivity or compulsivity also report greater difficulty with intrusive thoughts (Gay et al., 2011; Gillan et al., 2016). Clinically, persistent intrusive thoughts and action stopping deficits co-occur in numerous disorders: Obsessive thoughts and compulsive actions in obsessive-compulsive disorder (Fineberg et al., 2018; Gillan et al., 2017); intrusive memories and impaired response inhibition in PTSD (Falconer et al., 2008; Sadeh et al., 2018; Sadeh et al., 2015; van Rooij & Jovanovic, 2019; Wu et al., 2015); persistent worry and impulsivity in anxiety disorders (Berg et al., 2015) and intrusive thoughts and compulsivity in addiction (Everitt & Robbins, 2016; Kavanagh et al., 2005; May et al., 2015). These co-morbid deficits may reflect dysfunction in the rDLPFC, the rVLPFC or in other shared components of their control pathways. On the other hand, dissociations should arise when dysfunction selectively disrupts a domain-specific pathway linking rLPFC to target sites involved in generating actions and thoughts, including dysfunction to local inhibition at the target site itself. For example, individual variation in local GABAergic inhibition within the hippocampus or M1 predict inhibitory control over memories and actions, respectively, independently of prefrontal function (He et al., 2019; Schmitz et al., 2017). Thus, selective difficulties in action stopping or thought inhibition may arise, given focal deficits in either motor cortical or hippocampal GABA (Schmitz et al., 2017). The separate contributions of domain-general and domain-specific factors to inhibitory control implied by dynamic targeting constrains the utility of motor inhibition as a metric of inhibitory control over thought and may explain the surprisingly small SSRT deficits in major depression and anxiety, relative to attention deficit hyperactivity disorder or obsessive-compulsive disorder (Lipszyc & Schachar, 2010).

The current study did not seek to characterise the polysynaptic pathways through which the rDLPFC and rVLPFC suppress activity in either M1 or the hippocampus (Anderson et al., 2016; Depue et al., 2016). Rather, we focused on the existence of a central, domain-general inhibitory control function capable of flexibly shifting its top-down influence across actions and thoughts. By juxtaposing two well characterised model systems for stopping actions and thoughts, each with distinct neural targets of inhibition, we were able to show that the same set of prefrontal regions is involved in stopping processing in different cortical target areas, in a rapid, flexible manner. In doing so, we established evidence for dynamic inhibitory targeting as a key mechanism of domain-general inhibitory control in the human brain. More broadly, this work suggests that the human capacity for self-control in the face of life's challenges may emerge from a common wellspring of control over our actions and thoughts.

## Methods

We used a dataset from a published study (Schmitz et al., 2017). However, here all data were independently re-analysed with a different focus.

## Participants

Thirty right-handed native English speakers participated. Participants gave written informed consent and received money for participating. Five participants did not reach the 40% learning criterion on the Think/No-Think task, and one fell asleep during fMRI acquisition. The final sample comprised 24 participants (7 males, 17 females), 19-36 years old ( $M = 24.67$  years,  $SD = 4.31$ ). Participants had normal or corrected-to-normal vision and no reported history of neurological, medical, or memory disorders, and they were asked not to consume psychostimulants, drugs, or alcohol before the experiment. The Cambridge Psychology Research Ethics Committee approved the project.

## Experimental paradigm

Participants performed adapted versions of the Stop-signal (Logan & Cowan, 1984) and Think/No-Think (Anderson & Green, 2001) tasks. Both tasks require participants to stop unwanted processes, but in the motor and memory domains, respectively.

The Stop-signal task assesses the ability to stop unwanted actions. Participants first learn stimulus-response associations and then perform speeded motor responses to the presented (Go) stimuli. Occasionally, shortly after the Go stimulus, a stop signal occurs, and participants must withhold their response. We measured the stop-signal reaction time (SSRT), an estimate of how long it takes the participant to stop.

The Think/No-Think task assesses the ability to stop unwanted memory retrievals. Participants first form associations between unrelated cue-target word pairs. Then participants receive two-thirds of the cues as reminders (one at a time) and are asked to either think (Think items) or to not-think (No-Think items) of the associated target memory, with each Think and No-Think reminder repeated numerous times throughout the task. Finally, participants attempt to recall all initially learned associations. Typically, recall performance suffers for No-Think items compared to Baseline items that were neither retrieved nor suppressed during the think/no-think phase. This phenomenon, known as suppression-induced forgetting (SIF), indirectly measures the ability to stop unwanted memory retrievals by quantifying inhibitory aftereffects of this process (Anderson & Hanslmayr, 2014; Anderson & Weaver, 2009).

## Stimuli and apparatus

We presented stimuli and recorded responses with Presentation software (Neurobehavioral Systems, Albany, CA, USA). For the Stop-signal task, four visually discriminable red, green, blue, and yellow coloured circles of 2.5 cm in diameter, presented on a grey background, constituted the Go stimuli (Figure 2a). Participants responded by pressing

1 one of the two buttons (left or right) with a dominant 57  
2 (right) hand on a button box. An auditory 1000 Hz “beep” 58  
3 tone presented at a comfortable volume for 100 ms signalled 59  
4 participants to stop their responses. A fixation cross 60  
5 appeared in 50-point black Arial Rounded font on a grey 61  
6 background prior to the onset of the Go stimulus. 62

7 For the Think/No-Think task, we constructed 78 weakly 63  
8 relatable English word pairs (cue-target words, e.g., Part- 64  
9 Bowl) as stimuli and an additional 68 semantically related 65  
10 cue words for 68 of the target words (e.g., a cue word 66  
11 ‘Cornflake’ for the target word ‘Bowl’). We used 60 of the 67  
12 target words and their related and weak cues in the critical 68  
13 task, with the other items used as fillers. We divided the 69  
14 critical items into three lists composed of 20 targets and 70  
15 their corresponding weak cue words (the related word 71  
16 cues were set aside to be used as independent test cues 72  
17 on the final test; see procedure). We counterbalanced 73  
18 these lists across the within-subjects experimental 74  
19 conditions (Think, No-Think, and Baseline) so that across 75  
20 all participants, every pair participated equally often in 76  
21 each condition. We used the filler words both as practice 77  
22 items and also to minimise primacy and recency effects 78  
23 in the study list (Murdock, 1962). Words appeared in a 79  
24 32-point Arial font in capital letters on a grey background 80  
25 (Figure 2b). During the initial encoding and final recall 81  
26 phases, we presented all cues and targets in black. For the 82  
27 Think/No-Think phase, we presented the Think cues in 83  
28 green and the No-Think cues in red, each preceded by a 84  
29 fixation cross in 50-point black Arial Rounded font on a 85  
30 grey background. 86

### 31 **Procedure**

32 The procedure consisted of seven steps: 1) stimulus- 88  
33 response learning for the Stop-signal task; 2) Stop-signal 89  
34 task practice; 3) encoding phase of the Think/No-Think 90  
35 task; 4) Think/No-Think practice; 5) practice of inter- 91  
36 leaved Stop-signal and Think/No-Think tasks; 6) experi- 92  
37 mental phase during fMRI acquisition; 7) recall phase of 93  
38 the Think/No-Think task. We elaborate these steps below 94  
(see also Figure 2c). 95

### 40 **Step 1 – Stop-signal task stimulus-response learning**

41 Participants first formed stimulus-response associations for 97  
42 the Stop-signal task. As Go stimuli, we presented circles 98  
43 in four different colours (red, green, blue, and yellow) 99  
44 and participants had to respond by pressing one of the 100  
45 two buttons depending on the circle’s colour. Thus, each 101  
46 response button had two colours randomly assigned to it 102  
47 and participants associated each colour to its particular 103  
48 response. 104

49 Participants learned the colour-button mappings in two 105  
50 sets of two colours, with the first colour in a set associated 106  
51 with one button, and the second with the other button. 107  
52 After practising the responses to these colours in random 108  
53 order 10 times each, the same training was done on the 109  
54 second set. Subsequently, participants practised the colour- 110  
55 button mappings of all four colours in random order until 111  
56 they responded correctly to each colour on 10 consecutive 112

trials. During the practice, we instructed participants to respond as quickly and accurately as possible and provided feedback for incorrect or slow (> 1000 ms) responses.

### 57 **Step 2 – Stop-signal task practice**

58 Once participants learned the stimulus-response associations, 59  
59 we introduced the Stop-signal task. We instructed 60  
60 participants to keep responding to each coloured circle 61  
61 as quickly and accurately as possible but indicated that 62  
62 on some trials, after the circle appeared, a beep would 63  
63 sound, and that they should not press any button on these 64  
64 trials. We also told participants to avoid slowing down and 65  
65 waiting for the beep, requesting instead that they treat 66  
66 failures to stop as normal and always keep responding 67  
67 quickly and accurately. Thus, on Go trials, participants 68  
68 responded as quickly as possible, whereas, on Stop trials, 69  
69 a tone succeeded the cue onset, signalling participants to 70  
70 suppress their response. To facilitate performance, partici- 71  
71 pants received on-screen feedback for incorrect and too 72  
72 slow (> 700 ms) responses to Go trials, and for pressing 73  
73 a button on Stop trials.

74 Figure 2a presents the trial timings. Go trials started 75  
75 with a fixation cross, presented for 250 ms, followed by 76  
76 a coloured circle until response or for up to 2500 ms. 77  
77 After the response and a jittered inter-trial interval ( $M = 750$  ms,  $SD = 158.7$  ms), a new trial commenced. Stop 78  
78 trials proceeded identically except that a tone sounded 79  
79 shortly after the circle appeared. This stop signal delay 80  
80 varied dynamically in 50 ms steps (starting with 250 ms 81  
81 or 300 ms) according to a staircase tracking algorithm 82  
82 to achieve approximately a 50% success-to-stop rate for 83  
83 each participant. Note that the longer the stop signal 84  
84 delay is, the harder it is to not press the button. The 85  
85 dynamic tracking algorithm reduces participants’ ability to 86  
86 anticipate stop signal delay timing and provides a method 87  
87 for calculating the SSRT. In this practice step, participants 88  
88 performed 96 trials, of which 68 (71%) were Go trials and 89  
89 28 (29%) were Stop trials.

### 90 **Step 3 – Think/No-Think task encoding phase**

91 Once participants had learned the Stop-signal task, we 92  
92 introduced the Think/No-Think task. In the encoding 93  
93 phase, participants formed associations between 60 critical 94  
94 weakly-related word pairs (e.g., Part-Bowl) and between 95  
95 18 filler pairs. First, participants studied each cue-target 96  
96 word pair for 3.4 s with an inter-stimulus interval of 600 97  
97 ms. Next, from each studied pair, participants saw the cue 98  
98 word only and recalled aloud the corresponding target. 99  
99 We presented each cue for up to 6 s or until a response 100  
100 was given. Six hundred ms after cue offset, regardless 101  
101 of whether the participant recalled the item, the correct 102  
102 target appeared for 1 s. We repeated this procedure until 103  
103 participants recalled at least 40% of the critical pairs (all 104  
104 but 5 participants succeeded within the maximum of three 105  
105 repetitions). Finally, to assess which word-pairs participants 106  
106 learned, each cue word appeared again for 3.3 s with an 107  
107 inter-stimulus interval of 1.1 s and participants 108  
108 recalled aloud the corresponding target. We provided no 109  
109 feedback for incorrect responses.

1 feedback on this test.

2 **Step 4 – Think/No-Think practice**

3 After participants encoded the word pairs, the Think/No-  
4 Think practice phase commenced. On each trial, a cue  
5 word appeared on the screen in either green or red. We  
6 instructed participants to recall and think of the target  
7 words for cues presented in green (Think condition) but  
8 to suppress the recall and avoid thinking of the target  
9 words for those cues presented in red (No-Think condition).  
10 Participants performed the direct suppression variant  
11 of the Think/No-Think task (Benoit & Anderson, 2012;  
12 Bergström et al., 2009) in which, after reading and com-  
13 prehending the cue, they suppressed all thoughts of the  
14 associated memory without engaging in any distracting  
15 activity or thoughts. We asked participants to “push the  
16 memory out of mind” whenever it intruded.

17 Trial timings appear in Figure 2b. A trial consisted of  
18 presenting a cue in the centre of the screen for 3 s, followed  
19 by an inter-stimulus interval (0.5 s, M = 2.3 s, SD = 1.7  
20 s) during which we displayed a fixation cross. We jittered  
21 the inter-stimulus interval (0.5 s, M = 2.3 s, SD = 1.7  
22 s) to optimize the event-related design (as determined by  
23 optseq2: <http://surfer.nmr.mgh.harvard.edu/optseq>). In  
24 this practice phase, we used 12 filler items, six of which  
25 were allocated to the Think condition and six to the No-  
26 Think condition. We presented each item three times  
27 in random order (36 trials in total). In the middle of  
28 the practice, we administered a diagnostic questionnaire  
29 to ensure participants had understood and followed the  
30 instructions.

31 **Step 5 – Interleaved Stop-signal and Think/No-Think  
32 practice**

33 Before moving into the MRI scanner, participants per-  
34 formed an extended practice phase interleaving the Stop-  
35 signal and Think/No-Think tasks. For the Think/No-Think  
36 task, we again used 12 filler items. Other than that, and  
37 the fact that the practice took place outside the MRI scanner,  
38 this phase was identical to a single fMRI acquisition  
39 session described into more detail next.

40 **Step 6 – Experimental phase and fMRI acquisition**

41 In the main experimental phase, participants underwent  
42 8 fMRI scanning runs in a single session. Before the scan-  
43 ning began, participants saw the correct button-colour  
44 mappings and all 78 word pairs briefly presented on the  
45 screen to remind them of the task and items. After the brief  
46 refresher, the fMRI acquisition started. During each fMRI  
47 run, participants performed 8 blocks of the Think/No-  
48 Think task interleaved with 8 blocks of the Stop-signal  
49 task. All blocks lasted 30 s. To minimize carry-over ef-  
50 ffects, we interspersed 4 s rest periods (blank screen with a  
51 grey background) between blocks. Each block began with  
52 items that we did not score (the filler items) to reduce  
53 task-set switching effects between blocks. Within each  
54 block, we pseudo-randomly ordered all trials, and the trial  
55 timings for both tasks were identical to those used in their  
56 respective practice phases (step 2 and step 4; Figure 2a

57 58 59 60 61 62 63 64 65 66 67 68 69 70 71 72 73 74 75 76 77 78 79 80 81 82 83 84 85 86 87 88 89 90 91 92 93 94 95 96 97 98 99 100 101 102 103 104 105 106 107 108 109 110 111 112 113

Figure 2b).

50 Four of the Stop-signal task blocks contained Go trials  
51 only. We did not use these blocks in this report. Each  
52 of the other four Stop-signal blocks contained 12 trials,  
53 yielding 384 trials in total (8 runs \* 4 blocks per run \*  
54 12 trials per block). On average, across participants, Stop  
55 trials constituted 32% (SD = 2%) of the trials. As in the  
56 practice phase, a staircase tracking algorithm varied the  
57 delay between cue onset and stop-signal tone according  
58 to each participant’s performance, keeping the stopping  
59 success at approximately 50%.

60 Each of the Think/No-Think blocks contained 6 trials,  
61 starting with a filler item as a Think trial followed by  
62 5 Think or No-Think items in a pseudo-random order.  
63 Within each fMRI run, participants saw all 20 critical Think  
64 and 20 critical No-Think items once. Thus, across the 8  
65 runs, participants recalled or suppressed each memory  
66 item 8 times. The proportion of the Think trials (58%)  
67 exceeded the proportion of the No-Think trials (42%) to  
68 better resemble the higher frequency of Go trials than Stop  
69 trials during the Stop-signal task. We accomplished this by  
70 assigning Think trials to the filler items, without changing  
71 the frequency of Think trials on critical experimental items.  
72 After the fourth (middle) run, to allow participants to rest,  
73 we acquired their anatomical scan and administered the  
74 diagnostic questionnaire to ensure that participants closely  
75 followed the instructions of the Think/No-Think task.

76 **Step 7 – Think/No-Think recall phase**

77 In the final step (inside the scanner but without any scan  
78 acquisition), we measured the aftereffects of memory re-  
79 trieval and suppression via a cued-recall task on all word  
80 pairs (encoded in step 3). This included 20 Baseline items  
81 that were neither retrieved nor suppressed during the  
82 Think/No-Think phase and that thus provided a baseline  
83 estimate of the memorability of the pairs.

84 To reinstate the context of the initial encoding phase,  
85 we first tested participants on 10 filler cue words, 6 of  
86 which they had not seen since the encoding phase (step 3)  
87 and 4 of which they saw during the interleaved Stop-signal  
88 and Think/No-Think practice phase (step 5). We warned  
89 participants that the cues in this phase could be ones they  
90 had not seen for a long time and encouraged them to think  
91 back to the encoding phases to retrieve targets.

92 Following context reinstatement, participants per-  
93 formed the same-probe and independent-probe memory  
94 tests. In the same-probe test, we probed memory with the  
95 original cues (e.g. the weakly related cue word ‘Part’ for  
96 the target word ‘Bowl’). We included the independent-  
97 probe test to test whether forgetting generalized to novel  
98 cues (Anderson and Green, 2001), using the related cues  
99 we had designed for each target. For example, we cued  
100 with the semantic associate of the memory and its first  
101 letter (e.g., ‘Cornflake – B’ for the target ‘Bowl’). Across  
102 participants, we counterbalanced the order in which the  
103 tests appeared. In both tests, cues appeared for a maxi-  
104 mum of 3.3 s or until participants gave a response, with  
105 an inter-stimulus interval of 1.1 s. We coded a response as  
106 107 108 109 110 111 112 113

1 correct if participants correctly recalled the target while  
2 the cue was onscreen.  
57

3 Finally, we debriefed participants, and administered a  
4 post-experimental questionnaire to capture participants'  
5 experiences and the strategies they used in the Think/No-  
6 Think and Stop-signal tasks.  
62

## 7 Brain image acquisition

8 We collected MRI data using a 3-Tesla Siemens Tim Trio  
9 MRI scanner (Siemens, Erlangen, Germany) fitted with  
10 a 32-channel head coil. Participants underwent eight  
11 functional runs of the blood-oxygenation-level-dependent  
12 (BOLD) signal acquisitions. We acquired functional brain  
13 volumes using a gradient-echo, T2\*-weighted echoplanar  
14 pulse sequence (TR = 2000 ms, TE = 30 ms, flip angle  
15 = 90°, 32 axial slices, descending slice acquisition, voxel  
16 resolution = 3 mm<sup>3</sup>, 0.75 mm interslice gap). We dis-  
17 carded the first four volumes of each session to allow for  
18 magnetic field stabilisation. Due to technical problems  
19 encountered during task performance, we discarded from  
20 the analysis one functional run from two participants each,  
21 and two functional runs from another participant. After  
22 the fourth functional run, we acquired an anatomical refer-  
23 ence for each participant, a high-resolution whole-brain  
24 3D T1-weighted magnetization-prepared rapid gradient  
25 echo (MP-RAGE) image (TR = 2250 ms, TE = 2.99 ms,  
26 flip angle = 9°, field of view = 256 x 240 x 192 mm, voxel  
27 resolution = 1 mm<sup>3</sup>). Following the acquisition of the  
28 anatomical scan, participants underwent the remaining  
29 four functional runs.  
78

## 30 Data analysis

### 31 Behavioural performance

32 For statistical analyses of the behavioural data, we  
33 used R (v4, 2020-04-24) in Jupyter Notebook (Ana-  
34 conda, Inc., Austin, Texas). The data and detailed  
35 analysis notebook are freely available at <http://bit.do/analysis-domain-general>. For all statistical comparisons,  
36 we adopted  $p < 0.05$  as the significance threshold.  
37

38 For correlation analyses, we followed recommendations  
39 by Pernet et al. (2013) and used one of three correlation  
40 methods depending on whether the data were normally  
41 distributed or contained outliers. If there were no out-  
42 liers and data were normally distributed, we performed  
43 Pearson correlation and reported it as ' $r$ '. If there were  
44 univariate outliers (but no bivariate) or data were not  
45 normally distributed, we performed robust 20% Bend cor-  
46 relation and reported it as ' $r_{pp}$ '. If there were bivariate  
47 outliers, we performed robust Spearman skipped corre-  
48 lation using the minimum covariance determinant (MCD)  
49 estimator and reported it as ' $r_{ss}$ '. For univariate and bi-  
50 variate outlier detection, we used boxplot and bagplot  
51 methods, respectively.  
108

52 For the analysis of Stop-signal task data, we followed  
53 the guidelines by Verbruggen et al. (2019) and calculated  
54 SSRT using the integration method with the replacement  
55 of Go omissions. Specifically, we included all Stop trials  
56 and all Go trials (correct and incorrect), replacing missed  
109 trials with the maximum Go RT. To identify the nth  
110 fastest Go RT, we multiplied the number of total Go trials  
111 by the probability of responding to stop signal (unsuccess-  
112 ful stopping). The difference between the nth fastest Go  
113 RT and the mean SSD provided our estimate of SSRT.  
114

50 Go responses with the maximum Go RT. To identify the nth  
51 fastest Go RT, we multiplied the number of total Go trials  
52 by the probability of responding to stop signal (unsuccess-  
53 ful stopping). The difference between the nth fastest Go  
54 RT and the mean SSD provided our estimate of SSRT.  
55

56 In addition to SSRT, we calculated the probability of  
57 Go omissions, probability of choice errors on Go trials,  
58 probability of responding to Stop trials, mean SSD of all  
59 Stop trials, mean correct Go RT, and mean failed Stop RT.  
60 We also compared RTs of all Go trials against RTs of failed  
61 Stop trials to test the assumption of an independent race  
62 between a go and a stop runner. Besides, we assessed the  
63 change of Go RTs across the eight experimental blocks.  
64 Prior work suggests that the experiment-wide integration  
65 method can result in underestimation bias of SSRT if par-  
66 ticipants slow their RT gradually across experimental runs.  
67 In that case, a blocked integration method would provide  
68 a better measure of SSRT (Verbruggen et al., 2013). In our  
69 data, however, on average within the group, we observed  
70 a negligible decrease in RT across runs ( $B = -2.555$ ,  $p =$   
71 .250), suggesting that the experiment-wide integration  
72 method was more appropriate.  
73

74 For the Think/No-Think task data, we focused on the  
75 critical measure: SIF. We used the final recall scores (from  
76 step 7) of No-Think and Baseline items conditionalized on  
77 correct initial training performance (at step 3), as in prior  
78 work (Anderson et al., 2004). Thus, in the final recall  
79 scores, we did not include items that were not correctly  
80 recalled ( $M = 29\%$ ,  $SD = 17$ ) during the criterion test  
81 of the encoding phase, as the unlearned items can be  
82 neither suppressed nor retrieved during the Think/No-  
83 Think phase (step 6). As in our previous work (Schmitz et  
84 al., 2017), we averaged the scores across the same-probe  
85 and independent-probe tests and the difference between  
86 the Baseline and No-think item recall scores constituted  
87 our measure of SIF. To assess the group effect of SIF, we  
88 tested the data for normality ( $W = 0.95$ ,  $p = 0.264$ ) and  
89 performed a one-sample, one-sided t-test to determine  
90 if SIF is greater than zero. Finally, to assess whether  
91 inhibition ability generalises across motor and memory  
92 domains, we performed a correlation between the SSRT  
93 and SIF scores.  
94

95 To identify univariate and bi-variate outliers in the SSRT  
96 and SIF scores, we used box plot method, which relies  
97 on the interquartile range. Univariate outliers were not  
98 present for any of the two measures. One bi-variate out-  
99 lier was removed from the correlation analysis and the  
100 behavioural partial least squares analysis (described be-  
101 low). Nevertheless, outlier removal did not qualitatively  
102 alter the results.  
103

### 104 Brain imaging data

105 **Pre-processing.** We pre-processed and analysed the brain  
106 imaging data using Statistical Parametric Mapping v12 re-  
107 lease 7487 (SPM12; Wellcome Trust Centre for Neuroim-  
108 aging, London) in MATLAB vR2012a (The MathWorks, MA,  
109 USA). To approximate the orientation of the standard Mon-  
110 treal Neurological Institute (MNI) coordinate space, we re-  
111

1 oriented all acquired MRI images to the anterior-posterior 58  
2 commissure line and set the origins to the anterior com- 59  
3 missure. Next, we applied our pre-processing procedure 60  
4 to correct for head movement between the scans (images 61  
5 realigned to the mean functional image) and to adjust 62  
6 for temporal differences between slice acquisitions (slice- 63  
7 time correction relative to the middle axial slice). The 64  
8 procedure then co-registered each participant's anatomical 65  
9 image to the mean functional image and segmented 66  
10 it into grey matter, white matter, and cerebrospinal fluid. 67  
11 We then submitted the segmented images for each par- 68  
12 ticipant to the DARTEL procedure (Ashburner, 2007) to 69  
13 create a group-specific anatomical template which optim- 70  
14 ises inter-participant alignment. The DARTEL procedure 71  
15 alternates between computing a group template and warp- 72  
16 ing an individual's tissue probability maps into alignment 73  
17 with this template and ultimately creates an individual 74  
18 flow field of each participant. Subsequently, the procedure 75  
19 transformed the group template into MNI-152 space. Fi- 76  
20 nally, we applied the MNI transformation and smoothing 77  
21 with an 8 mm full-width-at-half-maximum (FWHM) Gaus- 78  
22 sian kernel to the functional images for the whole-brain 79  
23 voxel-wise analysis.

24 **Univariate whole-brain analysis.** To identify brain areas 81  
25 engaged in both inhibiting actions and inhibiting memo- 82  
26 ries, we performed a whole-brain voxel-wise univariate 83  
27 analysis. We high-pass filtered the time series of each voxel 84  
28 in the normalised and smoothed images with a cut-off fre- 85  
29 quency of 1/128 Hz, to remove low-frequency trends, and 86  
30 modelled for temporal autocorrelation across scans with 87  
31 the first-order autoregressive (AR(1)) process. We then 88  
32 submitted the pre-processed data of each participant to the 89  
33 first-level, subject-specific, General Linear Model (GLM) 90  
34 modelling a single design matrix for all functional runs. 91

35 We modelled the Stop-signal task and Think/No-Think 92  
36 task conditions as boxcar functions, convolved with a 93  
37 haemodynamic response function (HRF). In the model, 94  
38 we used group average response latencies for each trial 95  
39 type as the trial durations for the Stop-signal task con- 96  
40 dition, but we used 3 s epochs for the Think/No-Think 97  
41 task condition. As in the behavioural analysis, we condi- 98  
42 tionalized the Think and No-Think conditions on initial 99  
43 encoding performance. The main conditions of interest 100  
44 for our analysis included: correct Stop, correct Go (from 101  
45 the mixed Stop-signal and Go trial blocks only), condi- 102  
46 tionalized No-Think and conditionalized Think. Unlearned 103  
47 No-Think and Think items, filler items, incorrect Stop, 104  
48 incorrect Go and Go trials from the Go-only blocks we 105  
49 modelled as separate regressors of no interest. We also 106  
50 included the six realignment parameters for each run as 107  
51 additional regressors of no interest, to account for head 108  
52 motion artefacts, and a constant regressor for each run. 109  
53 We obtained the first-level contrast estimates for Stop, Go, 110  
54 No-Think, and Think conditions, and the main effect of 111  
55 Inhibit [Stop, No-Think] > Respond [Go, Think]. 112

56 At the second-level random-effect group analysis we 113  
57 entered the first-level contrast estimates of Stop, Go, No- 114

5 Think, and Think conditions into a repeated-measures 6 analysis of variance (ANOVA), which used pooled error and 7 correction for non-sphericity, with participants as between- 8 subject factor. We then performed a conjunction analysis 9 of Stop > Go No-Think > Think contrasts, using the 10 minimum statistics analysis method implemented in SPM12, 11 and testing the conjunction null hypothesis (Friston et 12 al., 2005; Nichols et al., 2005). The results of the 13 conjunction analysis represent voxels that were significant 14 for each individual contrast thresholded at  $p < 0.05$  false 15 discovery rate (FDR) corrected for whole-brain multiple 16 comparisons.

17 **Behavioural partial least squares (PLS) analysis.** We 18 hypothesised that domain-general inhibitory control brain 19 activity would be related to domain-general inhibitory 20 behaviour. To test our hypothesis, we performed behavioural 21 PLS analysis (Krishnan et al., 2011; McIntosh & Lobaugh, 22 2004) following a previously employed strategy (Gagne- 23 pain et al., 2017). We restricted our analysis to an inde- 24 pendent domain-general inhibitory control mask derived 25 from a meta-analytic conjunction analysis of 40 Stop-signal 26 and 16 Think/No-Think fMRI studies (described below). 27 Within this mask, we identified voxels where the BOLD 28 signal from the main effect of Inhibit > Respond contrast 29 depicted the largest joint covariance with the SSRT and 30 SIF scores.

31 Specifically, Inhibit > Respond contrast values from each 32 voxel of an MNI-normalised brain volume were aligned 33 and stacked across participants into a brain activation 34 matrix X, and SSRT and SIF scores were entered into a 35 matrix Y. In both matrices, rows represented participants. 36 We then individually mean-centred the X and Y matrices 37 and normalised each row in the matrix X (representing 38 each participant's voxel activations) so that the row sum 39 of squares equalled to one. Setting an equal variance of 40 voxel 41 activities across subjects ensured that the observed 42 differences between participants were not due to overall 43 differences in activation. Hereafter, a correlation of X and 44 Y matrices produced a matrix R encoding the relation- 45 ship between each voxel activity and behavioural scores 46 across participants. We then applied a singular-value 47 decomposition to the correlation matrix R to identify LVs 48 that maximise the covariance between voxel activation (X) 49 and behavioural measurements (Y). Each LV contained 50 a single value for each participant representing the 51 variance explained by the LV, and brain saliences, which are 52 a weighted pattern across brain voxels representing the 53 strength of the relationship between the BOLD signal and 54 the behavioural scores.

55 To assess the statistical significance of each LV and the 56 robustness of voxel saliences, we used 5000 permutation 57 tests and 5000 bootstrapped resamples, respectively. By 58 dividing each voxel's initial salience by the standard error of 59 its bootstrapped distribution, we obtained a bootstrapped 60 standard ratio, equivalent to a z-score, to assess the signifi- 61 cance of a given voxel. We thresholded the acquired scores 62 at 1.96, corresponding to  $p < 0.05$ , two-tailed. The multi- 63

1 variate PLS analysis method does not require correction 58  
2 for multiple comparisons as it quantifies the relationship 59  
3 between the BOLD signal and behavioural scores in a single 60  
4 analytic step (McIntosh & Lobaugh, 2004). 61

5 **Dynamic causal modelling (DCM) analysis.** We conducted 62  
6 a DCM analysis (Friston et al., 2003) to determine 63  
7 the most likely inhibition-related interactions between 64  
8 domain-general inhibitory control areas in the right pre- 65  
9 frontal cortex and domain-specific target areas. For the 66  
10 domain-specific target areas, we selected the left primary 67  
11 motor cortex (M1) and right hippocampus, based on our 68  
12 previous findings showing that stopping actions and stopping 69  
13 memories preferentially downregulates M1 and hippocampus, 70  
14 respectively (Schmitz et al., 2017). 71

15 DCM enables one to investigate hypothesised interactions 72  
16 among pre-defined brain regions by estimating the 73  
17 effective connectivity according to (1) the activity of other 74  
18 regions via intrinsic connections; (2) modulatory influences 75  
19 on connections arising through experimental manipulations; 76  
20 and (3) experimentally defined driving inputs to one or more of the 77  
21 regions (Friston et al., 2003). The intrinsic, modulatory, and 78  
22 driving inputs one specifies 79  
23 constitute the model structure assumed to represent the 80  
24 hypothesised neuronal network underlying the cognitive 81  
25 function of interest. 82

26 With DCM, a set of models can be defined that embody 83  
27 alternate hypotheses about the average connectivity and 84  
28 conditional moderation of connectivity. These models are 85  
29 inverted to the data and then compared in terms of the 86  
30 relative model evidence using Bayesian model selection 87  
31 (BMS). The differential model evidence from BMS indicates 88  
32 the probability that a given model is more likely to 89  
33 have generated the data than the other models and allows 90  
34 to infer both the presence and direction of modulatory 91  
35 connections. This can be estimated for individual models, 92  
36 or families of models that share critical features. 93

37 For the DCM analysis, we defined four regions of interest 94  
38 (ROIs): the right dorsolateral prefrontal cortex (rDLPFC), 95  
39 the right ventrolateral prefrontal cortex (rVLPFC), the 96  
40 right hippocampus, and the left M1. We obtained the 97  
41 rDLPFC and rVLPFC ROIs, centred at MNI coordinates 35, 98  
42 45, 24 and 44, 21, -1, respectively, from an independent 99  
43 meta-analytic conjunction analysis (described below). We 100  
44 defined the M1 ROI (centred at MNI coordinates -33, -22, 101  
45 -46) from a group analysis (N = 30) of an independent 102  
46 M1 localiser study on different participants (Button Press 103  
47 > View contrast). We mapped the rDLPFC, rVLPFC, and 104  
48 M1 ROIs from the MNI space to participants' native space. 105  
49 We manually traced the hippocampal ROIs in native space 106  
50 for each participant, using ITK-SNAP ([www.itksnap.org](http://www.itksnap.org); 107  
51 Yushkevich et al., 2006) and following established anatomical 108  
52 guidelines (Duvernoy et al., 2013; Pruessner et al., 109  
53 2000). Within each subject-specific ROI, we identified all 110  
54 significant voxels (thresholded at  $p < 0.05$ , uncorrected 111  
55 for multiple comparisons) for that participant based on the 112  
56 main effect of interest, which included Stop, Go, No-Think, 113  
57 and Think conditions. Only the identified significant voxels 114  
58

els were included in the final ROIs for the DCM analysis.

We performed the DCM analysis on participants' native-space, unsmoothed brain images, to maximise the anatomical specificity of the hand-traced hippocampal ROI. We estimated a first-level GLM for each participant in their native space. The GLM model was closely similar to the first-level model defined for the univariate whole-brain analysis (see above). But in this new model, we concatenated all functional runs into a single run to form a single time series per participant. Because we concatenated the runs, we did not model conditions that started less than 24 s before the end of each run (apart from the very last run), and we did not use the SPM high-pass filtering and temporal autocorrelation options, but as additional regressors of no interest we included sines and cosines of up to three cycles per run to capture low-frequency drifts, and regressors modelling each run.

From each of the four ROIs, we extracted the first eigenvariate of the BOLD signal time-course, adjusted for effects of interest. Based on these data, we estimated and compared a null model with no modulatory connections and 72 models with modulatory connections (73 models in total) to test alternative hypotheses about how suppressing actions and memories modulate connectivity between the four ROIs (see Figure 6a). All 72 models with modulatory connections were variants of the same basic model with intrinsic bidirectional connections between all regions except no intrinsic connections between M1 and hippocampus, and with driving inputs from the Stop-signal (Stop and Go trials) and Think/No-Think (No-Think and Think trials) tasks into both rDLPFC and rVLPFC regions. Across models, we varied the modulatory influences on the intrinsic connections arising through Stop or No-Think trials.

We grouped the 72 models into three families differing according to whether the source-target modulation was bidirectional, top-down, or bottom-up. Within each family, we defined four subfamilies that differed according to how Stop and No-Think trials modulate the prefrontal control and inhibitory target pathways: independent modulation of target regions by rDLPFC and rVLPFC (testing the idea that two parallel inhibition pathways might exist); rDLPFC only modulation (testing the idea that only rDLPFC supports inhibition); rVLPFC only modulation (testing the idea that only rVLPFC supports inhibition); or modulation of both rDLPFC and rVLPFC (testing the idea that both contribute to inhibition). Within the four subfamilies, we defined further four subfamilies according to how Stop and No-Think trials modulate interactions between the rDLPFC and rVLPFC regions: no interactions; rVLPFC modulates rDLPFC; rDLPFC modulates rVLPFC; or bidirectional interaction between rDLPFC and rVLPFC.

Furthermore, within each subfamily, we defined two additional subfamilies according to whether Stop and No-Think trials modulate the prefrontal connectivity with the preferred targets (M1 when stopping actions and hippocampus when stopping memories) or with the non-preferred targets (hippocampus when stopping actions and M1 when stopping memories), testing the idea that

1 inhibitory modulation must affect a task appropriate structure to model the data well. 58  
2

3 We compared the model evidence for the 73 models 60  
4 (the null model and 72 models with modulatory connec- 61  
5 tions) and the groups and subgroups of families across 62  
6 the 24 subjects using random-effects BMS (Penny et al., 63  
7 2010; Stephan et al., 2010). BMS reports the exceedance 64  
8 probability, which is a probability that a given model, or 65  
9 family of models, is more likely than any other model or 66  
10 family tested, given the group data. 67

11 **Multi-voxel pattern analysis.** We performed multi-voxel 68  
12 pattern analysis (MVPA) to test whether action and mem- 69  
13 ory inhibition share a common voxel activation pattern 70  
14 within an ROI. We used linear discriminant analysis (LDA) 71  
15 to classify voxel activity patterns within the same four 72  
16 ROIs that we used for the DCM analysis (rDLPFC, rVLPFC, 73  
17 right hippocampus, and left M1). 74

18 For each participant on their native-space unsmoothed 75  
19 brain images, we estimated a first-level GLM which was 76  
20 identical to the first-level model defined for the univariate 77  
21 whole-brain analysis (see above). The estimated beta 78  
22 weights of the voxels in each ROI were extracted and pre- 79  
23 whitened to construct noise normalized activity patterns 80  
24 for each event of interest (No-Think, Think, Stop, Go) 81  
25 within each of the eight functional fMRI runs. 82

26 To increase the reliability of pattern classification ac- 83  
27 curacy, we used a random subset approach (Diedrichsen 84  
28 et al., 2013). Specifically, for each ROI separately, we cre- 85  
29 ated up to 2000 unique subsets of randomly drawn 90% 86  
30 of ROI voxels (for smaller ROIs, there were less than 2000 87  
31 possible combinations). We then applied the LDA on each 88  
32 subset and averaged the subset results to obtain the final 89  
33 classification accuracy for each ROI. We performed two 90  
34 types of pattern classification to identify domain-general 91  
35 and domain-specific components within each ROI. 92

36 For the domain-general component, we performed a 93  
37 cross-task classification. We trained the LDA classifier to 94  
38 distinguish Inhibit from Respond conditions in one modal- 95  
39 ity (e.g. No-Think from Think) and tested whether the 96  
40 trained classifier could distinguish Inhibit from Respond 97  
41 in the other modality (e.g. Stop from Go). Both training 98  
42 and testing data consisted of two (conditions) by eight 99  
43 (runs) activation estimates for a set of voxels (e.g. 13 x 16 100  
44 matrix for a set of 13 voxels). For training and testing sets 101  
45 separately, for each voxel, we z-scored the activity pat- 102  
46 tterns across the 16 activation estimates setting the mean 103  
47 activity within each voxel to zero. This way, each voxel 104  
48 represented only the relative contribution of Inhibit vs 105  
49 Respond conditions within the Think/No-Think and Stop- 106  
50 signal tasks. For each ROI subset, we performed the LDA 107  
51 twice. The first classifier trained to discriminate Think 108  
52 from No-Think and returned the accuracy of distinguishing 109  
53 Stop from Go; the second classifier trained to discriminate 110  
54 Stop from Go and returned the accuracy of distinguishing 111  
55 Think from No-Think. The final score was the average clas-  
56 sification accuracy of all subsets and the two classification  
57 variants (up to 2000 x 2) per ROI and subject.

For the domain-specific component, we trained and tested the LDA classifier to distinguish No-Think from Stop conditions. The input data consisted of two (conditions) by eight (runs) activation estimates for a set of voxels. We z-scored the activity patterns across voxels for each event of interest. Thus, the mean ROI activity for each event was zero, and each voxel represented only its relative contribution to the given event. That way, we accounted for the univariate intensity differences between No-Think and Stop conditions. For each ROI subset, we performed leave-one-run out cross-validated LDA and averaged the classification accuracies across the eight cross-validation folds. The final score was the average classification accuracy of all subsets and cross-validation folds (up to 2000 x 8) per ROI and subject.

At the group level, for each ROI, we performed one-tailed t-tests to assess the statistical significance of classification accuracy being above the 50% chance level. All tests were Bonferroni corrected for the number of ROIs.

**A meta-analytic conjunction analysis of Stop-signal and Think/No-Think studies.** To acquire an independent mask of brain areas involved in domain-general inhibitory control, we updated a previously published meta-analysis of Stop-signal and Think/No-Think fMRI studies (Guo et al., 2018). The study selection process and included studies are reported in detail in (Guo et al., 2018). From the original meta-analysis, we excluded the current dataset (Schmitz et al., 2017) and included a different within-subjects (but with each task performed on different days) Stop-signal and Think/No-Think study from our lab (Guo, 2017). Consequently, our analysis included 40 Stop-signal and 16 Think/No-Think studies. We focused the meta-analysis on the conjunction of Stop > Go No-Think > Think contrasts which we conducted using Activation Likelihood Estimation (ALE) with GingerALE v3.0.2 (<http://www.brainmap.org/ale/>; Eickhoff et al., 2012; Eickhoff et al., 2017; Eickhoff et al., 2009; Turkeltaub et al., 2012). We used the same settings as reported before (Guo et al., 2018). Specifically, we used a less conservative mask size, a non-additive ALE method, no additional FWHM, and cluster analysis peaks at all extrema. In addition, we set the coordinate space to MNI152.

First, we conducted separate meta-analyses of Stop > Go, No-Think > Think, and their pooled data using cluster-level FWE corrected inference ( $p < 0.05$ , cluster-forming threshold uncorrected  $p < 0.001$ , threshold permutations = 1000). We then submitted the obtained thresholded ALE maps from the three individual meta-analyses to a meta-analytic contrast analysis (Eickhoff et al., 2011), which produced the conjunction of the Stop > Go & No-Think > Think contrasts. We thresholded the conjunction results at voxel-wise uncorrected  $p < 0.001$ , with the p-value permutations of 10,000 iterations, and the minimum cluster volume of 200 mm<sup>3</sup>.

## References

Anderson, M. C., Bunce, J. G., & Barbas, H. (2016). Prefrontal-hippocampal pathways underlying inhibitory control over memory. *Neurobiology of Learning and Memory*, 134, 145–161. <https://doi.org/10.1016/j.nlm.2015.11.008>

Anderson, M. C., & Green, C. (2001). Suppressing unwanted memories by executive control. *Nature*, 410(6826), 366–369. <https://doi.org/10.1038/35066572>

Anderson, M. C., & Hanslmayr, S. (2014). Neural mechanisms of motivated forgetting. *Trends in cognitive sciences*, 18(6), 279–92. <https://doi.org/10.1016/j.tics.2014.03.002>

Anderson, M. C., & Huddleston, E. (2012). Towards a cognitive and neurobiological model of motivated forgetting. In R. F. Belli (Ed.), *True and false recovered memories. nebraska symposium on motivation* (pp. 53–120). Springer. [https://doi.org/10.1007/978-1-4614-1195-6\\_3](https://doi.org/10.1007/978-1-4614-1195-6_3)

Anderson, M. C., & Hulbert, J. C. (2021). Active forgetting: Adaptation of memory by prefrontal control. *Annual Review of Psychology*, (In Press).

Anderson, M. C., Ochsner, K. N., Kuhl, B., Cooper, J., Robertson, E., Gabrieli, S. W., Glover, G. H., & Gabrieli, J. D. E. (2004). Neural systems underlying the suppression of unwanted memories. *Science*, 303(5655), 232–5. <https://doi.org/10.1126/science.1089504>

Anderson, M. C., & Weaver, C. (2009). Inhibitory control over action and memory. In L. Squire (Ed.), *Encyclopedia of neuroscience* (pp. 153–163). Academic Press. <https://doi.org/10.1016/B978-008045046-9.00421-6>

Aron, A. R. (2007). The neural basis of inhibition in cognitive control. *The Neuroscientist: a review journal bringing neurobiology, neurology and psychiatry*, 13(3), 214–28. <https://doi.org/10.1177/1073858407299288>

Aron, A. R., Fletcher, P. C., Bullmore, E. T., Sahakian, B. J., & Robbins, T. W. (2003). Stop-signal inhibition disrupted by damage to right inferior frontal gyrus in humans. *Nature neuroscience*, 6(2), 115–6. <https://doi.org/10.1038/nn1003>

Aron, A. R., & Poldrack, R. A. (2006). Cortical and subcortical contributions to stop signal response inhibition: Role of the subthalamic nucleus. *The Journal of Neuroscience*, 26(9), 2424–33. <https://doi.org/10.1523/JNEUROSCI.4682-05.2006>

Aron, A. R., Robbins, T. W., & Poldrack, R. A. (2004). Inhibition and the right inferior frontal cortex. *Trends in cognitive sciences*, 8(4), 170–7. <https://doi.org/10.1016/j.tics.2004.02.010>

Aron, A. R., Robbins, T. W., & Poldrack, R. A. (2014). Inhibition and the right inferior frontal cortex: One decade on. *Trends in cognitive sciences*, 18(4), 177–85. <https://doi.org/10.1016/j.tics.2013.12.003>

Ashburner, J. (2007). A fast diffeomorphic image registration algorithm. *NeuroImage*, 38(1), 95–113. <https://doi.org/10.1016/j.neuroimage.2007.07.007>

Badry, R., Mima, T., Aso, T., Nakatsuka, M., Abe, M., Fathi, D., Foley, N., Nagiub, H., Nagamine, T., & Fukuyama, H. (2009). Suppression of human cortico-motoneuronal excitability during the stop-signal task. *Clinical Neurophysiology*, 120(9), 1717–1723. <https://doi.org/10.1016/j.clinph.2009.06.027>

Banich, M. T., & Depue, B. E. (2015). Recent advances in understanding neural systems that support inhibitory control. *Current Opinion in Behavioral Sciences*, 1, 17–22. <https://doi.org/10.1016/j.cobeha.2014.07.006>

Bari, A., & Robbins, T. W. (2013). Inhibition and impulsivity: Behavioral and neural basis of response control. *Progress in Neurobiology*, 108, 44–79. <https://doi.org/10.1016/j.pneurobio.2013.06.005>

Benoit, R. G., & Anderson, M. C. (2012). Opposing mechanisms support the voluntary forgetting of unwanted memories. *Neuron*, 76(2), 450–460. <https://doi.org/10.1016/j.neuron.2012.07.025>

Benoit, R. G., Davies, D. J., & Anderson, M. C. (2016). Reducing future fears by suppressing the brain mechanisms underlying episodic simulation. *Proceedings of the National Academy of Sciences*, 113(52), E8492–E8501. <https://doi.org/10.1073/pnas.1606604114>

Benoit, R. G., Hulbert, J. C., Huddleston, E., & Anderson, M. C. (2015). Adaptive top-down suppression of hippocampal activity and the purging of intrusive memories from consciousness. *Journal of Cognitive Neuroscience*, 27(1), 96–111. [https://doi.org/10.1162/jocn\\_a\\_00696](https://doi.org/10.1162/jocn_a_00696)

Berg, J. M., Latzman, R. D., Bliwise, N. G., & Lilienfeld, S. O. (2015). Parsing the heterogeneity of impulsivity: A meta-analytic review of the behavioral implications of the upps for psychopathology. *Psychological Assessment*, 27(4), 1129–1146. <https://doi.org/10.1037/pas0000111>

Bergström, Z. M., de Fockert, J. W., & Richardson-Klavehn, A. (2009). Erp and behavioural evidence for direct suppression of unwanted memories. *NeuroImage*, 48(4), 726–37. <https://doi.org/10.1016/j.neuroimage.2009.06.051>

Botvinick, M. M. (2007). Conflict monitoring and decision making: Reconciling two perspectives on anterior cingulate function. *Cognitive, affective behavioral neuroscience*, 7(4), 356–66. <https://doi.org/10.3758/cabn.7.4.356>

Boucher, L., Palmeri, T. J., Logan, G. D., & Schall, J. D. (2007). Inhibitory control in mind and brain: An interactive race model of countermanding saccades. *Psychological Review*, 114(2), 376–397. <https://doi.org/10.1037/0033-295X.114.2.376>

Castiglione, A., Wagner, J., Anderson, M., & Aron, A. R. (2019). Preventing a thought from coming to mind elicits increased right frontal beta just as stopping action does. *Cerebral Cortex*, 29(5), 2160–2172. <https://doi.org/10.1093/cercor/bhz017>

Chambers, C. D., Bellgrove, M. A., Stokes, M. G., Henderson, T. R., Garavan, H., Robertson, I. H., Morris, A. P., & Mattingley, J. B. (2006). Executive "brake failure" following deactivation of human frontal lobe. *Journal of Cognitive Neuroscience*, 18(3), 444–455.

1 Chowdhury, N. S., Livesey, E. J., & Harris, J. A. (2019). 59  
2 Individual differences in intracortical inhibition during 60  
3 behavioural inhibition. *Neuropsychologia*, 124(August 61  
4 2018), 55–65. <https://doi.org/10.1016/j.neuropsychologia.2019.01.008> 63

5 Cocuzza, V. C., Ito, T., Schultz, D., Bassett, D. S., & Cole, 64  
6 M. W. (2020). Flexible coordinator and switcher hubs 65  
7 for adaptive task control. *The Journal of Neuroscience*, 66  
8 JN-RM-2559-19. [https://doi.org/10.1523/JNEUROSCI.](https://doi.org/10.1523/JNEUROSCI.67) 68  
9 2559-19.2020 68

10 Cole, M. W., Reynolds, J. R., Power, J. D., Repovs, G., An- 69  
11 aticevic, A., & Braver, T. S. (2013). Multi-task connectivity 70  
12 reveals flexible hubs for adaptive task control. *Nature* 71  
13 *Neuroscience*, 16(9), 1348–1355. <https://doi.org/10.1038/nn.3470> 73

14 Cole, M. W., & Schneider, W. (2007). The cognitive control 74  
15 network: Integrated cortical regions with dissociable 75  
16 functions. *NeuroImage*, 37(1), 343–360. <https://doi.org/10.1016/j.neuroimage.2007.03.071> 77

17 Cole, M. W., Yeung, N., Freiwalde, W. A., & Botvinick, M. 78  
18 (2009). Cingulate cortex: Diverging data from humans 79  
19 and monkeys. *Trends in Neurosciences*, 32(11), 566–574. 80  
20 <https://doi.org/10.1016/j.tins.2009.07.001> 81

21 Coxon, J. P., Stinear, C. M., & Byblow, W. D. (2006). In- 82  
22 tracortical inhibition during volitional inhibition of pre- 83  
23 paried action. *Journal of Neurophysiology*, 95(6), 3371– 84  
24 3383. <https://doi.org/10.1152/jn.01334.2005> 85

25 Crittenden, B. M., Mitchell, D. J., & Duncan, J. (2016). 86  
26 Task encoding across the multiple demand cortex is 87  
27 consistent with a frontoparietal and cingulo-opercular 88  
28 dual networks distinction. *The Journal of Neuroscience*, 89  
29 36(23), 6147–6155. <https://doi.org/10.1523/JNEUROSCI.4590-15.2016> 90

30 Depue, B. E., Orr, J. M., Smolker, H. R., Naaz, F., & Banich, 91  
31 M. T. (2016). The organization of right prefrontal net- 92  
32 works reveals common mechanisms of inhibitory regu- 93  
33 lation across cognitive, emotional, and motor processes. 94  
34 *Cerebral Cortex*, 26(4), 1634–1646. <https://doi.org/10.1093/cercor/bhu324> 95

35 Depue, B. E., Curran, T., & Banich, M. T. (2007). Prefrontal 96  
36 regions orchestrate via a two-phase process. *Science*, 97  
37 317(July), 215–219. 100

38 Diamond, A. (2013). Executive functions. *Annual Review* 101  
39 of *Psychology*, 64(1), 135–168. <https://doi.org/10.1146/annurev-psych-113011-143750> 103

40 Diedrichsen, J., Wiestler, T., & Ejaz, N. (2013). A multivari- 104  
41 ate method to determine the dimensionality of neural 105  
42 representation from population activity. *NeuroImage*, 106  
43 76, 225–235. <https://doi.org/10.1016/j.neuroimage.2013.02.062> 108

44 Dosenbach, N. U., Visscher, K. M., Palmer, E. D., Miezin, 109  
45 F. M., Wenger, K. K., Kang, H. C., Burgund, E. D., Grimes, 110  
46 A. L., Schlaggar, B. L., & Petersen, S. E. (2006). A core 111  
47 system for the implementation of task sets. *Neuron*, 112  
48 50(5), 799–812. <https://doi.org/10.1016/j.neuron.2006.04.031> 114

49 Duncan, J. (2010). The multiple-demand (md) system 115  
50 of the primate brain: Mental programs for intelligent 115

51 behaviour. *Trends in Cognitive Sciences*, 14(4), 172–179. 116  
52 <https://doi.org/10.1016/j.tics.2010.01.004>

53 Duvernoy, H. M., Cattin, F., & Risold, P.-Y. (2013). *The hu- 117  
54 man hippocampus: Functional anatomy, vascularization 118  
55 and serial sections with mri* (4th ed.). Springer Berlin 119  
56 Heidelberg. <https://doi.org/10.1007/978-3-642-33603-4>

57 Eickhoff, S. B., Bzdok, D., Laird, A. R., Kurth, F., & Fox, P. T. 120  
58 (2012). Activation likelihood estimation meta-analysis 121  
59 revisited. *NeuroImage*, 59(3), 2349–61. <https://doi.org/10.1016/j.neuroimage.2011.09.017>

60 Eickhoff, S. B., Bzdok, D., Laird, A. R., Roski, C., Caspers, 122  
61 S., Zilles, K., & Fox, P. T. (2011). Co-activation patterns 123  
62 distinguish cortical modules, their connectivity and func- 124  
63 tional differentiation. *NeuroImage*, 57(3), 938–49. <https://doi.org/10.1016/j.neuroimage.2011.05.021>

64 Eickhoff, S. B., Laird, A. R., Fox, P. M., Lancaster, J. L., & 125  
65 Fox, P. T. (2017). Implementation errors in the gingerale 126  
66 software: Description and recommendations. *Human 127  
67 brain mapping*, 38(1), 7–11. <https://doi.org/10.1002/hbm.23342>

68 Eickhoff, S. B., Laird, A. R., Grefkes, C., Wang, L. E., Zilles, 128  
69 K., & Fox, P. T. (2009). Coordinate-based activation 129  
70 likelihood estimation meta-analysis of neuroimaging 130  
71 data: A random-effects approach based on empirical 131  
72 estimates of spatial uncertainty. *Human brain mapping*, 132  
73 30(9), 2907–26. <https://doi.org/10.1002/hbm.20718>

74 Ersche, K. D., Jones, P. S., Williams, G. B., Turton, A. J., 133  
75 Robbins, T. W., & Bullmore, E. T. (2012). Abnormal 134  
76 brain structure implicated in stimulant drug addiction. 135  
77 *Science*, 335(6068), 601–604. <https://doi.org/10.1126/science.1214463>

78 Everitt, B. J., & Robbins, T. W. (2016). Drug addiction: 136  
79 Updating actions to habits to compulsions ten years 137  
80 on. *Annual Review of Psychology*, 67(1), 23–50. <https://doi.org/10.1146/annurev-psych-122414-033457>

81 Eysenck, M. W., Derakshan, N., Santos, R., & Calvo, M. G. 138  
82 (2007). Anxiety and cognitive performance: Attentional 139  
83 control theory. *Emotion*, 7(2), 336–353. <https://doi.org/10.1037/1528-3542.7.2.336>

84 Falconer, E., Bryant, R., Felmingham, K. L., Kemp, A. H., 140  
85 Gordon, E., Peduto, A., Olivieri, G., & Williams, L. M. 141  
86 (2008). The neural networks of inhibitory control in 142  
87 posttraumatic stress disorder. *Journal of psychiatry neuro- 143  
88 roscience : JPN*, 33(5), 413–22.

89 Fineberg, N. A., Apergis-Schoute, A. M., Vaghi, M. M., 144  
90 Banca, P., Gillan, C. M., Voon, V., Chamberlain, S. R., 145  
91 Cinosi, E., Reid, J., Shahper, S., Bullmore, E. T., Sahakian, 146  
92 B. J., & Robbins, T. W. (2018). Mapping compulsivity in 147  
93 the dsm-5 obsessive compulsive and related disorders: 148  
94 Cognitive domains, neural circuitry, and treatment. *Inter- 149  
95 national Journal of Neuropsychopharmacology*, 21(1), 150  
96 42–58. <https://doi.org/10.1093/ijnp/pyx088>

97 Fox, M. D., Snyder, A. Z., Vincent, J. L., Corbetta, M., 151  
98 Van Essen, D. C., & Raichle, M. E. (2005). From the 152  
99 cover: The human brain is intrinsically organized into 153  
100 dynamic, anticorrelated functional networks. *Proceed- 154*

ings of the National Academy of Sciences, 102(27), 9673–9678. <https://doi.org/10.1073/pnas.0504136102>

Friston, K. J., Harrison, L., & Penny, W. (2003). Dynamic causal modelling. *NeuroImage*, 19(4), 1273–302. [https://doi.org/10.1016/S1053-8119\(03\)00202-7](https://doi.org/10.1016/S1053-8119(03)00202-7)

Friston, K. J., Penny, W. D., & Glaser, D. E. (2005). Conjunction revisited. *NeuroImage*, 25(3), 661–667. <https://doi.org/10.1016/j.neuroimage.2005.01.013>

Gagnepain, P., Henson, R. N., & Anderson, M. C. (2014). Suppressing unwanted memories reduces their unconscious influence via targeted cortical inhibition. *Proceedings of the National Academy of Sciences of the United States of America*, 111(13), E1310–9. <https://doi.org/10.1073/pnas.1311468111>

Gagnepain, P., Hulbert, J., & Anderson, M. C. (2017). Parallel regulation of memory and emotion supports the suppression of intrusive memories. *The Journal of Neuroscience*, 37(27), 6423–6441. <https://doi.org/10.1523/JNEUROSCI.2732-16.2017>

Garavan, H., Ross, T. J., & Stein, E. a. (1999). Right hemispheric dominance of inhibitory control: An event-related functional mri study. *Proceedings of the National Academy of Sciences of the United States of America*, 96(14), 8301–6. <https://doi.org/10.1073/pnas.96.14.8301>

Gay, P., Schmidt, R. E., & Van der Linden, M. (2011). Impulsivity and intrusive thoughts: Related manifestations of self-control difficulties? *Cognitive Therapy and Research*, 35(4), 293–303. <https://doi.org/10.1007/s10608-010-9317-z>

Gillan, C. M., Fineberg, N. A., & Robbins, T. W. (2017). A trans-diagnostic perspective on obsessive-compulsive disorder. *Psychological Medicine*, 47(9), 1528–1548. <https://doi.org/10.1017/S0033291716002786>

Gillan, C. M., Kosinski, M., Whelan, R., Phelps, E. A., & Daw, N. D. (2016). Characterizing a psychiatric symptom dimension related to deficits in goal-directed control. *eLife*, 5. <https://doi.org/10.7554/eLife.11305>

Guo, Y. (2017). *The role of the basal ganglia in memory and motor inhibition* (Doctoral dissertation). University of Cambridge. <https://doi.org/10.17863/CAM.14695>

Guo, Y., Schmitz, T. W., Mur, M., Ferreira, C. S., & Anderson, M. C. (2018). A supramodal role of the basal ganglia in memory and motor inhibition: Meta-analytic evidence. *Neuropsychologia*, 108(November 2017), 117–134. <https://doi.org/10.1016/j.neuropsychologia.2017.11.033>

He, J. L., Fuelscher, I., Coxon, J., Chowdhury, N., Teo, W.-P., Barhoun, P., Enticott, P., & Hyde, C. (2019). Individual differences in intracortical inhibition predict motor-inhibitory performance. *Experimental Brain Research*, 237(10), 2715–2727. <https://doi.org/10.1007/s00221-019-05622-y>

Hu, X., Bergström, Z. M., Gagnepain, P., & Anderson, M. C. (2017). Suppressing unwanted memories reduces their unintended influences. *Current directions in psychological science*, 26(2), 197–206. <https://doi.org/10.1177/0963721417689881>

Jahanshahi, M., Obeso, I., Rothwell, J. C., & Obeso, J. A. (2015). A fronto-striato-subthalamic-pallidal network for goal-directed and habitual inhibition. *Nature Reviews Neuroscience*, 16(12), 719–732. <https://doi.org/10.1038/nrn4038>

Jana, S., Hannah, R., Muralidharan, V., & Aron, A. R. (2020). Temporal cascade of frontal, motor and muscle processes underlying human action-stopping. *eLife*, 9. <https://doi.org/10.7554/eLife.50371>

Ji, J. L., Spronk, M., Kulkarni, K., Repovš, G., Anticevic, A., & Cole, M. W. (2019). Mapping the human brain's cortical-subcortical functional network organization. *NeuroImage*, 185(September 2018), 35–57. <https://doi.org/10.1016/j.neuroimage.2018.10.006>

Joormann, J., & Tanovic, E. (2015). Cognitive vulnerability to depression: Examining cognitive control and emotion regulation. *Current Opinion in Psychology*, 4, 86–92. <https://doi.org/10.1016/j.copsyc.2014.12.006>

Kavanagh, D. J., Andrade, J., & May, J. (2005). Imaginary relish and exquisite torture: The elaborated intrusion theory of desire. *Psychological Review*, 112(2), 446–467. <https://doi.org/10.1037/0033-295X.112.2.446>

Krishnan, A., Williams, L. J., McIntosh, A. R., & Abdi, H. (2011). Partial least squares (pls) methods for neuroimaging: A tutorial and review. *NeuroImage*, 56(2), 455–475. <https://doi.org/10.1016/j.neuroimage.2010.07.034>

Kuhl, B. A., Dudukovic, N. M., Kahn, I., & Wagner, A. D. (2007). Decreased demands on cognitive control reveal the neural processing benefits of forgetting. *Nature Neuroscience*, 10(7), 908–914. <https://doi.org/10.1038/nn1918>

Levy, B. J., & Anderson, M. C. (2012). Purging of memories from conscious awareness tracked in the human brain. *Journal of Neuroscience*, 32(47), 16785–16794. <https://doi.org/10.1523/JNEUROSCI.2640-12.2012>

Levy, B. J., & Wagner, A. D. (2011). Cognitive control and right ventrolateral prefrontal cortex: Reflexive reorienting, motor inhibition, and action updating. *Annals of the New York Academy of Sciences*, 1224(1), 40–62. <https://doi.org/10.1111/j.1749-6632.2011.05958.x>

Lipszyc, J., & Schachar, R. (2010). Inhibitory control and psychopathology: A meta-analysis of studies using the stop signal task. *Journal of the International Neuropsychological Society*, 16(6), 1064–1076. <https://doi.org/10.1017/S1355617710000895>

Liu, Y., Lin, W., Liu, C., Luo, Y., Wu, J., Bayley, P. J., & Qin, S. (2016). Memory consolidation reconfigures neural pathways involved in the suppression of emotional memories. *Nature Communications*, 7, 1–12. <https://doi.org/10.1038/ncomms13375>

Logan, G. D., & Cowan, W. B. (1984). On the ability to inhibit thought and action: A theory of an act of control. *Psychological Review*, 91(3), 295–327. <https://doi.org/10.1037/0033-295X.91.3.295>

Marcus, D. S., Harwell, J., Olsen, T., Hodge, M., Glasser, M. F., Prior, F., Jenkinson, M., Laumann, T., Curtiss, S. W., & Van Essen, D. C. (2011). Informatics and data

1 mining tools and strategies for the human connectome 58  
2 project. *Frontiers in Neuroinformatics*, 5(June), 1–12. 59  
3 <https://doi.org/10.3389/fninf.2011.00004> 60  
4 Mary, A., Dayan, J., Leone, G., Postel, C., Fraisse, F., Malle, 61  
5 C., Vallée, T., Klein-Peschanski, C., Viader, F., de la 62  
6 Sayette, V., Peschanski, D., Eustache, F., & Gagnepain, 63  
7 P. (2020). Resilience after trauma: The role of mem- 64  
8 ory suppression. *Science*, 367(6479), eaay8477. <https://doi.org/10.1126/science.aay8477> 65  
9  
10 Mattia, M., Spadacenta, S., Pavone, L., Quarato, P., Es- 67  
11 posito, V., Sparano, A., Sebastian, F., Di Gennaro, G., 68  
12 Morace, R., Cantore, G., & Mirabella, G. (2012). Stop- 69  
13 event-related potentials from intracranial electrodes 70  
14 reveal a key role of premotor and motor cortices in stop- 71  
15 ping ongoing movements. *Frontiers in Neuroengineering*, 72  
16 5(June), 1–13. <https://doi.org/10.3389/fneng.2012.00012> 73  
17  
18 Matzke, D., Love, J., & Heathcote, A. (2017). A bayesian 75  
19 approach for estimating the probability of trigger failures 76  
20 in the stop-signal paradigm. *Behavior Research Methods*, 77  
21 49(1), 267–281. <https://doi.org/10.3758/s13428-015-0695-8> 78  
22  
23 Matzke, D., Love, J., Wiecki, V. T., Brown, S. D., Logan, 80  
24 G. D., & Wagenmakers, E. J. (2013). Release the beasts: 81  
25 Bayesian estimation of ex-gaussian stop-signal reaction 82  
26 time distributions. *Frontiers in Psychology*, 4(DEC), 1– 83  
27 13. <https://doi.org/10.3389/fpsyg.2013.00918> 84  
28 May, J., Kavanagh, D. J., & Andrade, J. (2015). The elabo- 85  
29 rated intrusion theory of desire: A 10-year retrospective 86  
30 and implications for addiction treatments. *Addictive Be- 87  
31 haviors*, 44, 29–34. <https://doi.org/10.1016/j.addbeh.2014.09.016> 88  
32  
33 McIntosh, A. R., & Lobaugh, N. J. (2004). Partial least 90  
34 squares analysis of neuroimaging data: Applications 91  
35 and advances. *NeuroImage*, 23(SUPPL. 1), 250–263. 92  
36 <https://doi.org/10.1016/j.neuroimage.2004.07.020> 93  
37 Murdock, B. B. (1962). The serial position effect of free 94  
38 recall. *Journal of Experimental Psychology*, 64(5), 482– 95  
39 488. <https://doi.org/10.1037/h0045106> 96  
40 Nichols, T., Brett, M., Andersson, J., Wager, T., & Poline, 97  
41 J. B. (2005). Valid conjunction inference with the mini- 98  
42 mum statistic. *NeuroImage*. <https://doi.org/10.1016/j.neuroimage.2004.12.005> 99  
43  
44 Nigg, J. T. (2017). Annual research review: On the re- 101  
45 lations among self-regulation, self-control, executive 102  
46 functioning, effortful control, cognitive control, impul- 103  
47 sivity, risk-taking, and inhibition for developmental psy- 104  
48 chopathology. *Journal of Child Psychology and Psychiatry*, 105  
49 58(4), 361–383. <https://doi.org/10.1111/jcpp.12675> 106  
50 Penny, W. D., Stephan, K. E., Daunizeau, J., Rosa, M. J., 107  
51 Friston, K. J., Schofield, T. M., & Leff, A. P. (2010). 108  
52 Comparing families of dynamic causal models. *PLoS 109  
53 computational biology*, 6(3), e1000709. <https://doi.org/10.1371/journal.pcbi.1000709> 110  
54  
55 Pernet, C. R., Wilcox, R., & Rousselet, G. A. (2013). Robust 112  
56 correlation analyses: False positive and power validation 113  
57 using a new open source matlab toolbox. *Frontiers in 114  
58*  
59  
60  
61  
62  
63  
64  
65  
66  
67  
68  
69  
70  
71  
72  
73  
74  
75  
76  
77  
78  
79  
80  
81  
82  
83  
84  
85  
86  
87  
88  
89  
90  
91  
92  
93  
94  
95  
96  
97  
98  
99  
100  
101  
102  
103  
104  
105  
106  
107  
108  
109  
110  
111  
112  
113  
114  
115  
116  
117  
118  
119  
120  
121  
122  
123  
124  
125  
126  
127  
128  
129  
130  
131  
132  
133  
134  
135  
136  
137  
138  
139  
140  
141  
142  
143  
144  
145  
146  
147  
148  
149  
150  
151  
152  
153  
154  
155  
156  
157  
158  
159  
160  
161  
162  
163  
164  
165  
166  
167  
168  
169  
170  
171  
172  
173  
174  
175  
176  
177  
178  
179  
180  
181  
182  
183  
184  
185  
186  
187  
188  
189  
190  
191  
192  
193  
194  
195  
196  
197  
198  
199  
200  
201  
202  
203  
204  
205  
206  
207  
208  
209  
210  
211  
212  
213  
214  
215  
216  
217  
218  
219  
220  
221  
222  
223  
224  
225  
226  
227  
228  
229  
230  
231  
232  
233  
234  
235  
236  
237  
238  
239  
240  
241  
242  
243  
244  
245  
246  
247  
248  
249  
250  
251  
252  
253  
254  
255  
256  
257  
258  
259  
260  
261  
262  
263  
264  
265  
266  
267  
268  
269  
270  
271  
272  
273  
274  
275  
276  
277  
278  
279  
280  
281  
282  
283  
284  
285  
286  
287  
288  
289  
290  
291  
292  
293  
294  
295  
296  
297  
298  
299  
300  
301  
302  
303  
304  
305  
306  
307  
308  
309  
310  
311  
312  
313  
314  
315  
316  
317  
318  
319  
320  
321  
322  
323  
324  
325  
326  
327  
328  
329  
330  
331  
332  
333  
334  
335  
336  
337  
338  
339  
340  
341  
342  
343  
344  
345  
346  
347  
348  
349  
350  
351  
352  
353  
354  
355  
356  
357  
358  
359  
360  
361  
362  
363  
364  
365  
366  
367  
368  
369  
370  
371  
372  
373  
374  
375  
376  
377  
378  
379  
380  
381  
382  
383  
384  
385  
386  
387  
388  
389  
390  
391  
392  
393  
394  
395  
396  
397  
398  
399  
400  
401  
402  
403  
404  
405  
406  
407  
408  
409  
410  
411  
412  
413  
414  
415  
416  
417  
418  
419  
420  
421  
422  
423  
424  
425  
426  
427  
428  
429  
430  
431  
432  
433  
434  
435  
436  
437  
438  
439  
440  
441  
442  
443  
444  
445  
446  
447  
448  
449  
450  
451  
452  
453  
454  
455  
456  
457  
458  
459  
460  
461  
462  
463  
464  
465  
466  
467  
468  
469  
470  
471  
472  
473  
474  
475  
476  
477  
478  
479  
480  
481  
482  
483  
484  
485  
486  
487  
488  
489  
490  
491  
492  
493  
494  
495  
496  
497  
498  
499  
500  
501  
502  
503  
504  
505  
506  
507  
508  
509  
510  
511  
512  
513  
514  
515  
516  
517  
518  
519  
520  
521  
522  
523  
524  
525  
526  
527  
528  
529  
530  
531  
532  
533  
534  
535  
536  
537  
538  
539  
540  
541  
542  
543  
544  
545  
546  
547  
548  
549  
550  
551  
552  
553  
554  
555  
556  
557  
558  
559  
560  
561  
562  
563  
564  
565  
566  
567  
568  
569  
570  
571  
572  
573  
574  
575  
576  
577  
578  
579  
580  
581  
582  
583  
584  
585  
586  
587  
588  
589  
590  
591  
592  
593  
594  
595  
596  
597  
598  
599  
600  
601  
602  
603  
604  
605  
606  
607  
608  
609  
610  
611  
612  
613  
614  
615  
616  
617  
618  
619  
620  
621  
622  
623  
624  
625  
626  
627  
628  
629  
630  
631  
632  
633  
634  
635  
636  
637  
638  
639  
640  
641  
642  
643  
644  
645  
646  
647  
648  
649  
650  
651  
652  
653  
654  
655  
656  
657  
658  
659  
660  
661  
662  
663  
664  
665  
666  
667  
668  
669  
670  
671  
672  
673  
674  
675  
676  
677  
678  
679  
680  
681  
682  
683  
684  
685  
686  
687  
688  
689  
690  
691  
692  
693  
694  
695  
696  
697  
698  
699  
700  
701  
702  
703  
704  
705  
706  
707  
708  
709  
710  
711  
712  
713  
714  
715  
716  
717  
718  
719  
720  
721  
722  
723  
724  
725  
726  
727  
728  
729  
730  
731  
732  
733  
734  
735  
736  
737  
738  
739  
740  
741  
742  
743  
744  
745  
746  
747  
748  
749  
750  
751  
752  
753  
754  
755  
756  
757  
758  
759  
760  
761  
762  
763  
764  
765  
766  
767  
768  
769  
770  
771  
772  
773  
774  
775  
776  
777  
778  
779  
780  
781  
782  
783  
784  
785  
786  
787  
788  
789  
790  
791  
792  
793  
794  
795  
796  
797  
798  
799  
800  
801  
802  
803  
804  
805  
806  
807  
808  
809  
8010  
8011  
8012  
8013  
8014  
8015  
8016  
8017  
8018  
8019  
8020  
8021  
8022  
8023  
8024  
8025  
8026  
8027  
8028  
8029  
8030  
8031  
8032  
8033  
8034  
8035  
8036  
8037  
8038  
8039  
8040  
8041  
8042  
8043  
8044  
8045  
8046  
8047  
8048  
8049  
8050  
8051  
8052  
8053  
8054  
8055  
8056  
8057  
8058  
8059  
8060  
8061  
8062  
8063  
8064  
8065  
8066  
8067  
8068  
8069  
8070  
8071  
8072  
8073  
8074  
8075  
8076  
8077  
8078  
8079  
8080  
8081  
8082  
8083  
8084  
8085  
8086  
8087  
8088  
8089  
8090  
8091  
8092  
8093  
8094  
8095  
8096  
8097  
8098  
8099  
80100  
80101  
80102  
80103  
80104  
80105  
80106  
80107  
80108  
80109  
80110  
80111  
80112  
80113  
80114  
80115  
80116  
80117  
80118  
80119  
80120  
80121  
80122  
80123  
80124  
80125  
80126  
80127  
80128  
80129  
80130  
80131  
80132  
80133  
80134  
80135  
80136  
80137  
80138  
80139  
80140  
80141  
80142  
80143  
80144  
80145  
80146  
80147  
80148  
80149  
80150  
80151  
80152  
80153  
80154  
80155  
80156  
80157  
80158  
80159  
80160  
80161  
80162  
80163  
80164  
80165  
80166  
80167  
80168  
80169  
80170  
80171  
80172  
80173  
80174  
80175  
80176  
80177  
80178  
80179  
80180  
80181  
80182  
80183  
80184  
80185  
80186  
80187  
80188  
80189  
80190  
80191  
80192  
80193  
80194  
80195  
80196  
80197  
80198  
80199  
80200  
80201  
80202  
80203  
80204  
80205  
80206  
80207  
80208  
80209  
80210  
80211  
80212  
80213  
80214  
80215  
80216  
80217  
80218  
80219  
80220  
80221  
80222  
80223  
80224  
80225  
80226  
80227  
80228  
80229  
80230  
80231  
80232  
80233  
80234  
80235  
80236  
80237  
80238  
80239  
80240  
80241  
80242  
80243  
80244  
80245  
80246  
80247  
80248  
80249  
80250  
80251  
80252  
80253  
80254  
80255  
80256  
80257  
80258  
80259  
80260  
80261  
80262  
80263  
80264  
80265  
80266  
80267  
80268  
80269  
80270  
80271  
80272  
80273  
80274  
80275  
80276  
80277  
80278  
80279  
80280  
80281  
80282  
80283  
80284  
80285  
80286  
80287  
80288  
80289  
80290  
80291  
80292  
80293  
80294  
80295  
80296  
80297  
80298  
80299  
80300  
80301  
80302  
80303  
80304  
80305  
80306  
80307  
80308  
80309  
80310  
80311  
80312  
80313  
80314  
80315  
80316  
80317  
80318  
80319  
80320  
80321  
80322  
80323  
80324  
80325  
80326  
80327  
80328  
80329  
80330  
80331  
80332  
80333  
80334  
80335  
80336  
80337  
80338  
80339  
80340  
80341  
80342  
80343  
80344  
80345  
80346  
80347  
80348  
80349  
80350  
80351  
80352  
80353  
80354  
80355  
80356  
80357  
80358  
80359  
80360  
80361  
80362  
80363  
80364  
80365  
80366  
80367  
80368  
80369  
80370  
80371  
80372  
80373  
80374  
80375  
80376  
80377  
80378  
80379  
80380  
80381  
80382  
80383  
80384  
80385  
80386  
80387  
80388  
80389  
80390  
80391  
80392  
80393  
80394  
80395  
80396  
80397  
80398  
80399  
80400  
80401  
80402  
80403  
80404  
80405  
80406  
80407  
80408  
80409  
80410  
80411  
80412  
80413  
80414  
80415  
80416  
80417  
80418  
80419  
80420  
80421  
80422  
80423  
80424  
80425  
80426  
80427  
80428  
80429  
80430  
80431  
80432  
80433  
80434  
80435  
80436  
80437  
80438  
80439  
80440  
80441  
80442  
80443  
80444  
80445  
80446  
80447  
80448  
80449  
80450  
80451  
80452  
80453  
80454  
80455  
80456  
80457  
80458  
80459  
80460  
80461  
80462  
80463  
80464  
80465  
80466  
80467  
80468  
80469  
80470  
80471  
80472  
80473  
80474  
80475  
80476  
80477  
80478  
80479  
80480  
80481  
80482  
80483  
80484  
80485  
80486  
80487  
80488  
80489  
80490  
80491  
80492  
80493  
80494  
80495  
80496  
80497  
80498  
80499  
80500  
80501  
80502  
80503  
80504  
80505  
80506  
80507  
80508  
80509  
80510  
80511  
80512  
80513  
80514  
80515  
80516  
80517  
80518  
80519  
80520  
80521  
80522  
80523  
80524  
80525  
80526  
80527  
80528  
80529  
80530  
80531  
80532  
80533  
80534  
80535  
80536  
80537  
80538  
80539  
80540  
80541  
80542  
80543  
80544  
80545  
80546  
80547  
80548  
80549  
80550  
80551  
80552  
80553  
80554  
80555  
80556  
80557  
80558  
80559  
80560  
80561  
80562  
80563  
80564  
80565  
80566  
80567  
80568  
80569  
80570  
80571  
80572  
80573  
80574  
80575  
80576  
80577  
80578  
80579  
80580  
80581  
80582  
80583  
80584  
80585  
80586  
80587  
80588  
80589  
80590  
80591  
80592  
80593  
80594  
80595  
80596  
80597  
80598  
80599  
80600  
80601  
80602  
80603  
80604  
80605  
80606  
80607  
80608  
80609  
80610  
80611  
80612  
80613  
80614  
80615  
80616  
80617  
80618  
80619  
80620  
80621  
80622  
80623  
80624  
80625  
80626  
80627  
80628  
80629  
80630  
80631  
80632  
80633  
80634  
80635  
80636  
80637  
80638  
80639  
80640  
80641  
80642  
80643  
80644  
80645  
80646  
80647  
80648  
80649  
80650  
80651  
80652  
80653  
80654  
80655  
80656  
80657  
80658  
80659  
80660  
80661  
80662  
80663  
80664  
80665  
80666  
80667  
80668  
80669  
80670  
80671  
80672  
80673  
80674  
80675  
80676  
80677  
80678  
80679  
80680  
80681  
80682  
80683  
80684  
80685  
80686  
80687  
80688  
80689  
80690  
80691  
80692  
80693  
80694  
80695  
80696  
80697  
80698  
80699  
80700  
80701  
80702  
80703  
80704  
80705  
80706  
80707  
80708  
80709  
80710  
80711  
80712  
80713  
80714  
80715  
80716  
80717  
80718  
80719  
80720  
80721  
80722  
80723  
80724  
80725  
80726  
80727  
80728  
80729  
80730  
80731  
80732  
80733  
80734  
80735  
80736  
80737  
80738  
80739  
80740  
80741  
80742  
80743  
80744  
80745  
80746  
80747  
80748  
80749  
80750  
80751  
80752  
80753  
80754  
80755  
80756  
80757  
80758  
80759  
80760  
80761  
80762  
80763  
80764  
80765<br

1 Stephan, K., Penny, W., Moran, R., den Ouden, H., Dau- 59  
2 nizeau, J., & Friston, K. (2010). Ten simple rules for dy- 60  
3 namic causal modeling. *NeuroImage*, 49(4), 3099–3109. 61  
4 <https://doi.org/10.1016/j.neuroimage.2009.11.015> 62

5 Stinear, C. M., Coxon, J. P., & Byblow, W. D. (2009). Pri- 63  
6 mary motor cortex and movement prevention: Where 64  
7 stop meets go. *Neuroscience and Biobehavioral Reviews*, 65  
8 33(5), 662–673. <https://doi.org/10.1016/j.neubiorev.2008.08.013> 66  
9

10 Sumitash, J., Ricci, H., Muralidharan, V., & Aron, A. R. 68  
11 (2019). Temporal cascade of frontal, motor and muscle 69  
12 processes underlying human action-stopping. *bioRxiv*, 70  
13 1–41. <https://doi.org/https://doi.org/10.1101/700088> 71

14 Swann, N. C., Tandon, N., Pieters, T. A., & Aron, A. R. 72  
15 (2013). Intracranial electroencephalography reveals dif- 73  
16 ferent temporal profiles for dorsal- and ventro-lateral 74  
17 prefrontal cortex in preparing to stop action. *Cerebral 75  
18 Cortex*, 23(10), 2479–2488. <https://doi.org/10.1093/cercor/bhs245> 76  
19

20 Turkeltaub, P. E., Eickhoff, S. B., Laird, A. R., Fox, 78  
21 M., Wiener, M., & Fox, P. (2012). Minimizing within- 79  
22 experiment and within-group effects in activation likeli- 80  
23 hood estimation meta-analyses. *Human brain mapping*, 81  
24 33(1), 1–13. <https://doi.org/10.1002/hbm.21186> 82

25 van den Wildenberg, W. P. M., Burle, B., Vidal, F., van 83  
26 der Molen, M. W., Ridderinkhof, K. R., & Hasbroucq, 84  
27 T. (2010). Mechanisms and dynamics of cortical motor 85  
28 inhibition in the stop-signal paradigm: A tms study. 86  
29 *Journal of Cognitive Neuroscience*, 22(2), 225–239. <https://doi.org/10.1162/jocn.2009.21248> 87  
30

31 van Rooij, S. J., & Jovanovic, T. (2019). Impaired inhibition 90  
32 as an intermediate phenotype for ptsd risk and treat- 91  
33 ment response. *Progress in Neuro-Psychopharmacology 91  
34 and Biological Psychiatry*, 89, 435–445. <https://doi.org/10.1016/j.pnpbp.2018.10.014> 92  
35

36 Verbruggen, F., Aron, A. R., Band, G. P., Beste, C., Bissett, 93  
37 P. G., Brockett, A. T., Brown, J. W., Chamberlain, S. R., 94  
38 Chambers, C. D., Colonius, H., Colzato, L. S., Corneil, 94  
39 B. D., Coxon, J. P., Dupuis, A., Eagle, D. M., Garavan, H., 94  
40 Greenhouse, I., Heathcote, A., Huster, R. J., ... Boehler, 94  
41 C. N. (2019). A consensus guide to capturing the ability 94  
42 to inhibit actions and impulsive behaviors in the stop- 94  
43 signal task. *eLife*, 8, 1–26. <https://doi.org/10.7554/elife.46323> 94  
44

45 Verbruggen, F., Chambers, C. D., & Logan, G. D. (2013). 94  
46 Fictitious inhibitory differences: How skewness and 94  
47 slowing distort the estimation of stopping latencies. *Psy- 94  
48 chological science*, 24(3), 352–62. <https://doi.org/10.1177/0956797612457390> 94  
49

50 Wessel, J. R., Conner, C. R., Aron, A. R., & Tandon, N. 94  
51 (2013). Chronometric electrical stimulation of right in- 94  
52 ferior frontal cortex increases motor braking. *Journal of 94  
53 Neuroscience*, 33(50), 19611–19619. <https://doi.org/10.1523/JNEUROSCI.3468-13.2013> 94  
54

55 Wiecki, V. T., & Frank, M. J. (2013). A computational 94  
56 model of inhibitory control in frontal cortex and basal 94  
57 ganglia. *Psychological Review*, 120(2), 329–355. <https://doi.org/10.1037/a0031542> 94  
58

59 Wimber, M., Alink, A., Charest, I., Kriegeskorte, N., & An- 94  
60 derson, M. C. (2015). Retrieval induces adaptive for- 94  
61 getting of competing memories via cortical pattern sup- 94  
62 pression. *Nature neuroscience*, 18(4), 582–9. <https://doi.org/10.1038/nn.3973> 94  
63

64 Wu, J., Yuan, Y., Cao, C., Zhang, K., Wang, L., & Zhang, L. 94  
65 (2015). The relationship between response inhibition 94  
66 and posttraumatic stress symptom clusters in adolescent 94  
67 earthquake survivors: An event-related potential study. 94  
68 *Scientific Reports*, 5(1), 8844. <https://doi.org/10.1038/srep08844> 94  
69

70 Yeo, B. T. T., Krienen, F. M., Eickhoff, S. B., Yaakub, S. N., 94  
71 Fox, P. T., Buckner, R. L., Asplund, C. L., & Chee, M. W. 94  
72 (2015). Functional specialization and flexibility in hu- 94  
73 man association cortex. *Cerebral Cortex*, 25(10), 3654– 94  
74 3672. <https://doi.org/10.1093/cercor/bhu217> 94  
75

76 Yushkevich, P. A., Piven, J., Hazlett, H. C., Smith, R. G., 94  
77 Ho, S., Gee, J. C., & Gerig, G. (2006). User-guided 3d 94  
78 active contour segmentation of anatomical structures: 94  
79 Significantly improved efficiency and reliability. *Neuro- 94  
80 Image*, 31(3), 1116–1128. <https://doi.org/10.1016/j.neuroimage.2006.01.015> 94  
81

82 Zandbelt, B. B., Bloemendaal, M., Hoogendam, J. M., Kahn, 94  
83 R. S., & Vink, M. (2013). Transcranial magnetic stimula- 94  
84 tion and functional mri reveal cortical and subcortical 94  
85 interactions during stop-signal response inhibition. 94  
86 *Journal of Cognitive Neuroscience*, 25(2), 157–174. [https://doi.org/10.1162/jocn\\_a\\_00309](https://doi.org/10.1162/jocn_a_00309) 94  
87

88 Zandbelt, B. B., & Vink, M. (2010). On the role of the 94  
89 striatum in response inhibition. *PLoS ONE*, 5(11). <https://doi.org/10.1371/journal.pone.0013848> 94  
90

91 Zhang, R., Geng, X., & Lee, T. M. C. (2017). Large-scale 94  
92 functional neural network correlates of response inhibi- 94  
93 tion: An fmri meta-analysis. *Brain Structure and Func- 94  
94 tion*, 222(9), 3973–3990. <https://doi.org/10.1007/s00429-017-1443-x> 94  
95